5

Earthquake-generated tsunami

INTRODUCTION

The most common cause of tsunami is seismic activity. Over the past two millennia, earthquakes have produced 82.3% of all tsunami in the Pacific Ocean. Displacement of the Earth's crust by several meters during underwater earthquakes may cover tens of thousands of square kilometers and impart tremendous potential energy to the overlying water. These types of events are common; however, tsunamigenic earthquakes are rare. Between 1861 and 1948, over 15,000 earthquakes produced only 124 tsunami. Along the west coast of South America, which is one of the most tsunami-prone coasts in the world, 1,098 offshore earthquakes have generated only 20 tsunami. This low frequency of occurrence may simply reflect the fact that most tsunami are small in amplitude and go unnoticed. Two-thirds of damaging tsunami in the Pacific Ocean region have been associated with earthquakes with a surface wave magnitude of 7.5 or more (Figure 5.1). The majority of these earthquakes have been teleseismic events affecting distant coastlines as well as local ones. One out of every three of these teleseismic events has been generated in the 20th century by earthquakes in Peru or Chile. This chapter discusses the mechanics of tsunamigenic earthquakes, and where possible, attempts to associate them with some of the signatures for tsunami presented in Chapter 3.

Seismic waves

(Geist, 1997b; Bryant, 2005)

Earthquakes occurring mainly in the upper 100 km of the ocean's crust generate tsunami. However, earthquakes centered over adjacent landmass have also produced tsunami. Earthquakes produce seismic waves transmitted through the Earth from an epicenter that can lie as deep as 700 km beneath the Earth's surface. These seismic waves consist of four types: *P*, *S*, Rayleigh, and Love waves. *P* waves are primary

Figure 5.1. Artist's impression of the second and largest tsunami smashing into the Alaska Railway terminus at Seward in Prince William Sound, March 27, 1964 (see color section). Locomotive 1828 was carried 50 m. Note that the locomotive has become a water-borne missile—a trait often generated by tsunami bores as described in Chapter 2. Drawing by Pierre Mion and appearing in December 1971 issue of *Popular Science*. *Source: http://www.alaskarails.org/historical/ earthquake/photos/tidal-wave.jpg*

waves that arrive first at a seismograph. The wave is compressional, consisting of alternating compression and dilation similar to waves produced by sound traveling through air. These waves can pass through gases, liquids, and solids. *P* waves can thus travel through the center of the Earth; however, at the core–mantle boundary, they are refracted, producing two 3,000 km wide shadow zones without any detectable *P* waves on the opposite side of the globe from an epicenter. To detect tsunami produced by earthquakes, seismic stations must be located outside these shadow zones. *S* or shear waves behave very much like the propagation of a wave down a skipping rope that has been shaken up and down. These waves travel 0.6 times slower than primary waves. The spatial distribution and time separation between the arrival of *P* and *S* waves at a seismograph station can be used to determine the location and magnitude of an earthquake. Love and Rayleigh waves spread slowly outward from the epicenter along the surface of the Earth's crust. Love waves have horizontal motion and are responsible for much of the damage witnessed during earthquakes. Rayleigh waves have both horizontal and vertical motions that produce an elliptical rotation of the ground similar to that produced in water particles by the passage of an ocean wave. While it is logical to believe that earthquakes generate tsunami through the physical displacement of the seabed along a fault line that breaches the seabed, tsunami also obtain their energy from Rayleigh waves.

MAGNITUDE SCALES FOR EARTHQUAKES AND TSUNAMI

Earthquake magnitude scales

(Bolt, 1978; Okal, Talandier, and Reymond, 1991; Schindelé *et al.*, 1995)

Earthquakes were originally measured using the Richter scale, M_L, defined as the logarithm to base ten of the maximum seismic wave amplitude recorded on a seismograph at a distance of 100 kilometers from an earthquake's epicenter. This scale saturates around a value of seven. A more useful scale measures the largest magnitude of seismic waves at the surface at a period of 20 seconds. This yields the surface wave magnitude, M_s. The M_s scale is so well recognized that it is commonly used to describe the size of tsunamigenic earthquakes. An M_s magnitude earthquake of 8.0 occurs about twice per year, but only 10% of these occur under an ocean with movement along a fault that is favorable for the generation of a tsunami. Earthquake-generated tsunami are associated with seismic events having an M_s magnitude of 7.0 or greater. Around the coast of Japan any shallow submarine earthquake with a magnitude greater than 7.3 will generate a tsunami. The tsunami period is also proportional to the magnitude of uplift. Small earthquakes tend to produce short tsunami wavelengths. Most tsunami-generating earthquakes are shallow and occur at depths in the Earth's crust between 0 km and 40 km.

Unfortunately, the M_s scale also saturates, this time around a magnitude of eight, precisely at the point where significant tsunami begin to form. A better measure of the size of an earthquake is its seismic moment, M_o, measured in Newton meters (N m)

and based upon the forces acting along a fault line. From this a moment magnitude, M_w, can be determined from long-period surface waves of more than 250 seconds using the following formula:

$$M_w = 0.67 \log_{10} M_o - 10.73 \tag{5.2}$$

where M_w = moment magnitude scale (dimensionless)
M_o = seismic moment

The moment magnitude does not saturate and gives a consistent measure across the complete span of earthquake sizes. Only large earthquakes, with a moment magnitude, M_w, greater than 8.6, can generate destructive teleseismic tsunami, ones that impact across an ocean basin.

Tsunami earthquakes

(Kanamori and Kikuchi, 1993; Okal, 1988, 1993; Beroza, 1995; Geist, 1997b)

The preceding scales imply that the size of a tsunami should increase as the magnitude of the earthquake increases. This is true for most teleseismic tsunami in the Pacific Ocean; however, it is now known that many earthquakes with small and moderate seismic moments can produce large, devastating tsunami. The Great Meiji Sanriku earthquake of 1896 and the Alaskan earthquake of April 1, 1946 were of this type. The Sanriku earthquake was not felt widely along the adjacent coastline, yet the tsunami that arrived 30 minutes afterwards produced run-ups that exceeded 30 m in places and killed 27,132 people. These types of events are known as tsunami earthquakes. Submarine landslides are thought to be one of the reasons some small earthquakes can generate large tsunami, but this explanation has not been proven conclusively. Submarine landslides as a cause of tsunami will be treated in more detail in Chapter 6. Presently, it is believed that slow rupturing along fault lines causes tsunami earthquakes. Only broadband seismometers, sensitive to low-frequency waves with wave periods greater than 100 seconds, can detect slow earthquakes that spawn "silent", killing tsunami. Figure 5.2 illustrates the difference between a

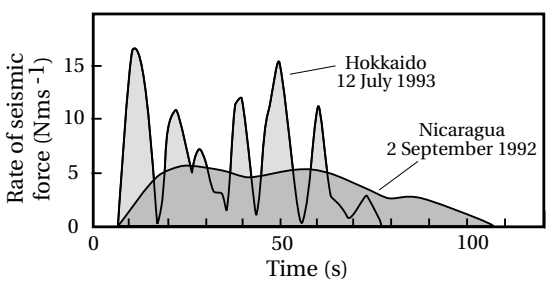

Figure 5.2. Comparison of the rate of seismic force between normal (Hokkaido) and slow (Nicaraguan) tsunamigenic earthquakes. Based on Kikuchi and Kanamori (1995).

Table 5.1. Disparity between the seismic magnitude, M_s, and the moment magnitude, M_w, of recent earthquakes illustrating tsunami earthquakes.

Event	*Date*	*Seismic magnitude* M_s	*Moment magnitude* M_w	*Maximum Run-up* (m)
Sanriku	June 15, 1896	7.2	8.0	38.2
Unimak Island, Alaska	April 1, 1946	7.4	8.2	35.0
Peru	November 20, 1960	6.8	7.6	9.0
Kuril Islands	October 20, 1963	6.9	7.8	15.0
Kuril Islands	June 10, 1975	7.0	7.5	5.5
Nicaragua	September 2, 1992	7.2	7.7	10.7
Java	June 2, 1994	7.2	7.7	13.9

Source: Based on Geist (1997b), and Intergovernmental Oceanographic Commission (1999).

tsunami earthquake and an ordinary one. The Hokkaido 1993 tsunami was an ordinary event. The earthquake that generated it lasted for about 80 seconds and consisted of five large and two minor shock waves. The earthquake was regionally felt along the northwest coast of Japan. It produced a deadly tsunami. In contrast, the Nicaraguan tsunami of 1992 had no distinct peak in seismic wave activity. Rather, the movement along the fault line occurred as a moderate disturbance, for at least 80 seconds, tapering off over the next half-minute. The earthquake was hardly felt along the nearby coast, yet it produced a killer tsunami. Both of these events will be described in detail later in this chapter.

The energy released by slow earthquakes can be measured accurately; however, the change is not rapid enough to trigger a substantive response using the M_s scale based upon surface wave detection algorithms. Instead, a potential tsunami earthquake can be detected better using the moment magnitude, M_w. Technically, tsunami earthquakes are ones that occur in the ocean where the difference between the M_s and M_w magnitudes is significantly large. Table 5.1 illustrates this difference for some modern tsunami. Besides the Sanriku and Alaskan events mentioned earlier, significant tsunami earthquakes occurred in the Kuril Islands on October 20, 1963, off Nicaragua on September 2, 1992, and off Java on June 2, 1994, with maximum run-ups of 15 m, 10.7 m, and 13.9 m respectively. Tsunami earthquakes happen with two conditions: where thick, accretional prisms develop at the junction of two crustal plates and wherever sediments are being subducted. Earthquakes under the former setting generated the 1896 Sanriku and 1946 Unimak Island tsunami. In contrast, the Peru, Kuril Islands, and Nicaragua tsunami listed in Table 5.1 were generated beneath subduction zones. The mechanisms of tsunami earthquake generation will be discussed in more detail later.

Tsunami magnitude scales

(Horikawa and Shuto, 1983; Abe, 1979, 1983; Hatori, 1986; Shuto, 1993)

Because of the high frequency of occurrence of tsunami around Japan, extensive research has been carried out there into predicting tsunami characteristics and magnitude. The following scale, known as the Imamura–Iida scale, was defined using approximately a hundred Japanese tsunami between 1700 and 1960:

$$m_{II} = \log_2 H_{r\max} \tag{5.3}$$

where m_{II} = Imamura–Iida's tsunami magnitude scale (dimensionless)
$H_{r\max}$ = maximum tsunami run-up height—Equations (2.11)–(2.13)

On the Imamura–Iida scale, the biggest tsunami in Japan—the Meiji Great Sanriku tsunami of 1896, which had a run-up height of 38.2 m—had a magnitude of 4.0. The other great Sanriku tsunami of 1933—which ranks as the second largest recorded tsunami in Japan—had a magnitude of 3.0. Japanese tsunami have between 1% and 10% of the total energy of the source earthquake. The relationship between the magnitude of an earthquake and the Imamura–Iida scale is presented in Table 5.2. Only earthquakes of magnitude 7.0 or greater are responsible for significant tsunami waves in Japan with run-up heights in excess of 1 m. However, as an earthquake's magnitude rises above 8.0, the run-up height and destructive energy of the wave dramatically increase. A magnitude 8.0 earthquake can produce a tsunami wave of between 4 m and 6 m in height. The magnitude needs to increase only to a value of 8.75 to generate the 38.2 m wave height of the Meiji Great Sanriku tsunami. The Imamura–Iida magnitude scale has now acquired worldwide usage. However,

Table 5.2. Earthquake magnitude, tsunami magnitude, and tsunami run-up heights in Japan.

Earthquake magnitude	*Tsunami magnitude*	*Maximum run-up* (m)
6.0	−2	<0.3
6.5	−1	0.5–0.75
7.0	0	1.0–1.5
7.5	1	2.0–3.0
8.0	2	4.0–6.0
8.3	3	8.0–12.0
8.5	4	16.0–24.0
8.8	5	>32.0

Source: Based on Iida (1963).

Table 5.3. Soloviev's scale of tsunami magnitude.

Earthquake magnitude	*Mean run-up height* (m)	*Maximum run-up height* (m)
−3.0	0.1	0.1
−2.0	0.2	0.2
−1.0	0.4	0.4
0.0	0.7	0.9
1.0	1.5	2.1
2.0	2.8	4.8
2.5	4.0	7.9
3.0	5.7	13.4
3.5	8.0	22.9
4.0	11.3	40.3
4.5	16.0	73.9

Source: Based on Iida (1963).

because the maximum run-up height of a tsunami can be so variable along a coast, Soloviev proposed a more general scale as follows:

$$i_s = \log_2(1.4H_r^-) \tag{5.4}$$

where i_s = Soloviev's tsunami magnitude (dimensionless)
H_r^- = mean tsunami run-up height along a stretch of coast (m)

This scale and its relationship to both mean and maximum tsunami run-up heights are summarized in Table 5.3. Neither the Imamura–Iida nor the Soloviev scales relate transparently to earthquake magnitude. For example, both tsunami scales contain negative numbers and peak around a value of 4.0. Most tsunami are also generated by earthquakes over a narrow range of magnitudes whereas the two tsunami scales span a broader range. Several attempts have been made to construct a more identifiable tsunami magnitude scale. Abe established one of the more widely used of these scales as follows:

$$M_t = \log_{10} H_r + 9.1 + \Delta C \tag{5.5}$$

where M_t = tsunami magnitude at a coast
ΔC = a small correction on tsunami magnitude dependent on source region

Average ΔC corrections for Hilo, California, and Japan are 0.3, 0.2, and 0.0, respectively, irrespective of the source region of the tsunamigenic earthquake. There have been 15 historical events in the Pacific Ocean with a tsunami magnitude greater than 8.5. The largest of these was the May 22, 1960 Chilean tsunami with an M_t value of 9.4. All Pacific-wide events have had a tsunami magnitude greater than 8.5. Ten of these events have occurred in the 20th century, with the latest originating in the Aleutian Islands on February 4, 1965. The tsunami magnitude scale has the advantage of being closely equated to the magnitude of earthquakes near their source because the average value of M_t for a coastline is set equal to the average M_w value of source earthquakes. Recently, emphasis has been placed upon near-field earthquakes and the M_t scale has been reformulated to include the exact distance between a coast and the epicenter of a tsunamigenic earthquake. For example, research on many tsunami on the east coast of Japan shows the following relationship:

$$M_t = \log_{10} H_r + \log_{10} R_e + 5.80 \tag{5.6}$$

where M_t = tsunami magnitude (dimensionless)
R_e = the shortest distance to the epicenter of a tsunamigenic earthquake (km)

The constant in this equation is dependent upon the source region. At present, few values have been calculated beyond Japanese waters, so there is no universal value that can be easily inserted into Equation (5.6). Tsunami waves clearly carry quantitative information about the details of earthquake-induced deformation of the seabed in the source region. Knowing the tsunami magnitude, M_t, it is possible to calculate the amount of seabed involved in its generation using the following formula:

$$M_t = \log_{10} S_t + 3.9 \tag{5.7}$$

where S_t = area of seabed generating a tsunami (m^2)

There is excellent agreement between the tsunami magnitudes calculated using Equations (5.5) and (5.7). Finally, the Imamura–Iida scale has been converted to a form similar to Equation (5.6) as follows:

$$m_{II} = 2.7(\log_{10} H_r + \log_{10} R_e) - 4.3 \tag{5.8}$$

SEISMIC GAPS AND TSUNAMI OCCURRENCE

(Satake, 1996; Bak, 1997; Bryant, 2005)

The concept of earthquake cycles depends upon crustal movement occurring at constant rates over geological time and the build-up of frictional drag along fault lines. Around the Pacific Rim, plates are moving at consistent rates. For instance, in the Alaskan region, the Pacific and North American Plates have generated continual earthquake activity over the past 150 years as stresses build up to crucial limits and are periodically released at various points along the plate margin. However, stresses may not be released at some points. These appear in the historical record as abnormally aseismic zones surrounded by seismically active regions. The former locations

are called seismic gaps and are believed to be prime sites for future earthquake activity. The Alaskan earthquake of 1964 filled in one of these gaps, and a major gap now exists in the Los Angeles area.

The seismic gap concept is flawed. Many earthquakes occur in swarms, with the leading earthquake not necessarily being the largest one. Tsunami generation also tends to occur in the area encompassing aftershocks. More significantly, when many tsunami events are examined, the arrival times of the first wave along different coastlines tend not to originate from a single point source. Finally, earthquakes and the tsunami they generate are chaotic geophysical phenomena. They should thus be generated by a spectrum of seismic waves with varying amplitudes and periods. If this is the case, then the system of tsunamigenic earthquakes behaves as white noise. One of the aspects of such systems is that earthquakes recur at the same location rather than in areas that are more quiescent. This behavior is characteristic of subduction zone earthquakes. For example, the October 4, 1994 Kuril Islands tsunami occurred at the same location as a previous event in 1969. A casual glance at the source location of tsunami over time in the Pacific will show that tsunami originate repetitively within a 100 km radius of the same location in many regions (Figure 1.2).

RELATIONSHIPS BETWEEN EARTHQUAKES AND TSUNAMI

How earthquakes generate tsunami

(Wiegel, 1970; Ben-Menahem and Rosenman, 1972; Ward, 1980; Okal, 1988; Satake, 1996; Geist, 1997b; Noson, Qamar, and Thorsen, 1988; Porter and Leeds, 2000; Carydis, 2004; Ellsworth *et al.*, 2004; National Geophysical Data Center, 2007)

Rupturing along active fault lines where two sections of the Earth's crust are moving opposite each other causes tsunamigenic earthquakes. Only three types of faults can generate a tsunami: a strike–slip earthquake on a vertical fault, a dip–slip earthquake on a vertical fault, and a thrusting earthquake on a dipping plane (Figure 5.3). In each case rupturing can occur at any point along a fault line deep in the Earth's crust. This location is known as the focal depth of the epicenter. The dip–slip and thrust fault line configurations are better at producing tsunami than the strike–slip pattern. While the dip–slip mechanism seems to be a logical one for tsunami generation because it abruptly displaces large sections of the seafloor vertically, the area of uplift cancels out the area of subsidence, resulting in small or non-existent tsunami. From a depth of 30 km below the seabed to the surface, the thrust fault, which is characteristic of subduction zones (Figure 5.3), becomes the preferred fault mechanism for tsunami generation. The greater the vertical displacement (or slip), then the greater the amplitude of the tsunami. About 90% of earthquakes occur in subduction zones and these areas are the prime source for tsunami. Subduction zones typically have average dips of $25^\circ \pm 9^\circ$, while the largest tsunami run-up is associated with higher dip values of between 20° and 30°. As the dip angle decreases, the tsunami is more likely to have a leading trough. Faulting along subduction zones also results in

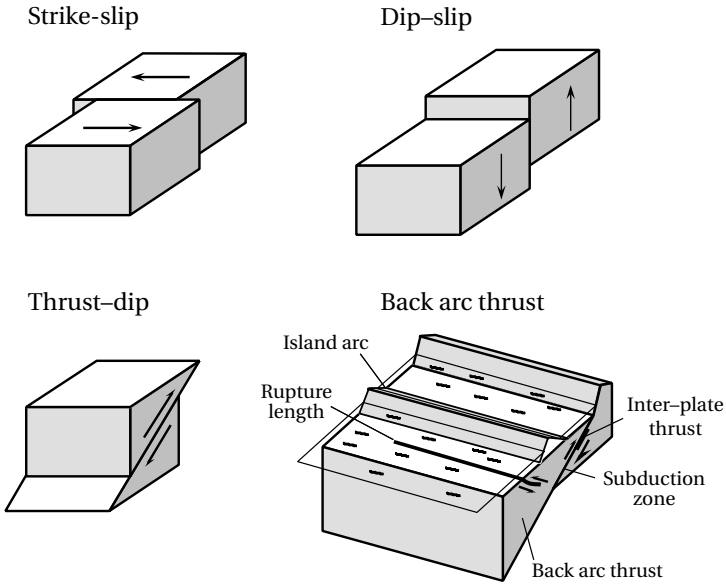

Figure 5.3. Types of faults giving rise to tsunami. Based on Okal (1988), and Geist (1997b).

subsidence at the coastline, a feature that compounds tsunami inundation for local earthquakes. Two tsunami actually develop in this case, one propagating shoreward and the other seaward. This tends to produce waveforms of different characteristics. The portion propagating seaward has a flatter crest and smaller amplitude than the wave moving landward. Large tsunami are not restricted to subduction zones. For example, back-arc thrusting away from a plate boundary (Figure 5.3) produced the Flores, Indonesia, tsunami of December 12, 1992 and the Hokkaido Nansei–Oki tsunami of July 12, 1993. In addition, the November 14, 1994 Mindoro, Philippines, tsunami, which killed 78 people, was generated along a strike–slip fault, while the October 4, 1994 Kuril Islands tsunami originated from the middle of a subducting slab. These anomalous events may also have involved a secondary mechanism such as a submarine landslide.

The greatest slip along faults tends to be concentrated toward the center of a rupture, and this can result in a higher initial tsunami. This abnormal amplitude may not be detected if the degree of slip along a fault is averaged. Tsunami earthquakes tend to have much greater slip displacement than tsunamigenic earthquakes of comparable magnitude (Figure 5.4). For example, slip displacement for a tsunamigenic earthquake with a moment magnitude, M_w, of 8.0 is only 2 m. The equivalent tsunami earthquake has a value that is more than double this. The length and orientation of a rupture are also important in the generation of a tsunami. Length obviously correlates with the amount of seafloor displacement. Analyses show that the amplitude of a tsunami is proportional to the cube of the length of rupturing. Long ruptures such as those that occur along the coast of South America have the

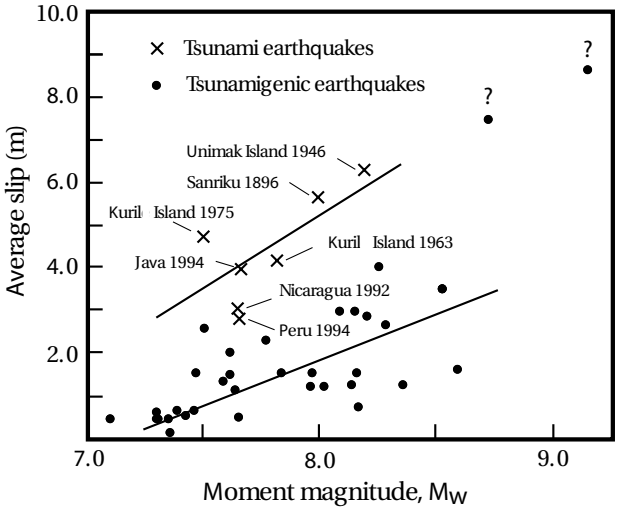

Figure 5.4. Relationship between moment magnitude, M_w, and the average slip distance of an earthquake. Based on Geist (1997b).

potential to produce the largest Pacific-wide tsunami. Rupturing over a 1,000 km length of fault line caused the exceptional 1960 Chilean tsunami. At the other extreme, if the tsunami wavelength that is generated by an earthquake is less than the rupture length, then there is a beaming effect. This certainly was the case with the Alaskan earthquake of 1964, whose tsunami concentrated along the Californian and Chilean coasts. The effect of beaming or directivity on a coastline depends upon its orientation relative to that of the rupturing fault line. Most subduction zones in the Pacific Ocean direct tsunami toward the center of the ocean. Thus, places like Hawaii and French Polynesia are particularly vulnerable. An exception to this occurs with tsunami originating in Alaska. Here most of the energy in a tsunami is beamed toward California and Chile. The east coasts of India and Sri Lanka received the full brunt of the Indian Ocean tsunami of December 2004 because they were orientated parallel to the rupture zone extending northward from Indonesia. Very little energy for this tsunami propagated into the southeastern Indian Ocean because this region lay in a shadow zone where beaming was minimal.

The velocity of a rupture can be calculated from the nature of seismic waves arriving at various seismographs. There is an inverse correlation between the rupture velocity and directivity. Note that tsunami earthquakes have low rupture speeds (about 1.0 km s^{-1} compared with 2.5 km s^{-1}–3.5 km s^{-1} for normal subduction zone earthquakes). Tsunami earthquakes therefore have higher directivity and so can produce higher wave run-up along narrow sections of a coast. In the Pacific Ocean, rupturing occurs along major subduction zones that parallel coastlines. Tsunami should thus propagate at right angles to the rupture, or directly into the center of the ocean. This is the reason islands such as Hawaii and French Polynesia are so

prone to teleseismic tsunami in the Pacific. An exception to this occurs along the Aleutian Island–Alaskan coastline. Here, fault lines are radial and project tsunami toward the Californian and Chilean coasts. As one goes westward along the Aleutian Island chain, the directivity of wave propagation sweeps toward Hawaii. Alaskan earthquakes do not affect French Polynesia because of topographic modification across the intervening ocean. For these reasons, once the epicenter of an earthquake has been located around the Pacific Rim, it is a simple task to plot the resulting tsunami's direction of travel and likely area of impact.

It is assumed that faulting occurs in massive rock units. Faulting is not this simple. In subduction zones, sedimentary rocks are often being buried. Accretional wedges can build up on the seabed as surface sediments are scraped off as one plate dips below another. This is especially prominent where low-angle trusting is occurring. Marine sediments are also water saturated. Close to continents these sediments can contain organic material that decomposes into methane, leading to gas-rich layers. Both of these types of sedimentary layers have low densities. Thrust rupturing into these types of sedimentary layers can increase the excitation of tsunami waves by a factor of 10. Only 10% of the force of the rupture needs to occur in the overlying sedimentary layer for this to happen. Tsunami earthquakes may also be generated by aftershocks associated with rupturing of an active fault through softer sediments near the seabed. In summary, the most prone area in the ocean for the generation of large tsunami is along a subduction zone where one plate moves upward over another at a low angle, and where this movement propagates through less consolidated sediments near the seabed. In these circumstances, while the moment magnitude, M_w, of the tsunamigenic earthquake may be an order of magnitude smaller than expected, the resulting tsunami can be very large.

There are two anomalies that have virtually been ignored in the tsunami literature. First, while it is generally perceived that tsunami can only be generated by earthquakes with an M_s magnitude of 7.0 or greater, reality is far different. One of the most definitive databases on tsunami is maintained by NOAA's National Geophysical Data Center (2007). It contains a record of 1,610 tsunami from 2000 BC to the present. Surprisingly, 50% of earthquakes with a magnitude below 7.1 have generated identifiable tsunami. Fifty-three earthquakes with a magnitude of 5.8 or less have produced tsunami. Measurements exist for only 33 of these events. This represents only 2% of known events. Despite the paucity of records, some of these small earthquakes have produced destructive tsunami. Twenty-five of the events generated tsunami that reached more than 1.0 m above sea level. Two earthquakes with magnitudes of 5.2 and 5.6 produced tsunami reaching 6.1 m and 6.0 m, respectively, above sea level. The first occurred in Southern California on August 31, 1930, while the latter occurred on the South Island of New Zealand on May 17, 1947.

Second, vertical ground motions caused mainly by the passage of Rayleigh seismic waves can generate tsunami-like effects. The tsunamigenic potential of such movements is poorly researched. There are numerous accounts of seiching or sloshing of water in small enclosed bodies of water or narrow channels such as estuaries and rivers following earthquakes with M_s magnitudes of 6 or less. When ground displacement linked to faulting is filtered out, the magnitude of vertical ground motions can

be substantial. For example, vertical ground motions exceeded 23.5 cm for the 6.7 M_w magnitude Northridge earthquake of January 17, 1994 (Ellsworth *et al.*, 2004) and 100 cm for the 7.9 M_w magnitude Denali earthquake of November 3, 2002 in Alaska (Porter and Leeds, 2000). These ground motions are large enough that they would have generated sizable tsunami had they occurred underwater. In western Europe, earthquakes are shallow and the effects of vertical motion are independent of earthquake magnitude. In Greece, earthquakes with magnitudes as low as 4.2 have generated vertical motion of 8 cm, enough to cause substantial building destruction. While this amplitude appears small, similar uplift of the seabed in confined bodies of water could generate tsunami that can not only cause noticeable effects, but also explain some of the reports of tsunami following small earthquakes. The possibility of small earthquakes generating significant tsunami has been underestimated.

Linking tsunami run-up to earthquake magnitude

(Iida, 1985)

For warning purposes, it is better to be able to predict the height of a tsunami along a coast given the magnitude of its source earthquake. Some tsunami approaching coasts tend to have a height that is consistent over long stretches of coastline. This certainly holds true along the east coast of Japan and the west coast of the United States. This fact can then be used to calculate the run-up height of a tsunami at various locations even if the slope varies—Equations (2.11)–(2.13). Figure 5.5 shows the relationships between the moment magnitude, M_w, of earthquakes and the amplitude of tsunami recorded on tide gauges for the east coast of Japan and Papeete, Tahiti in the middle of the South Pacific Ocean. The data sets take into account both near-field and distant earthquakes, and have the following linear

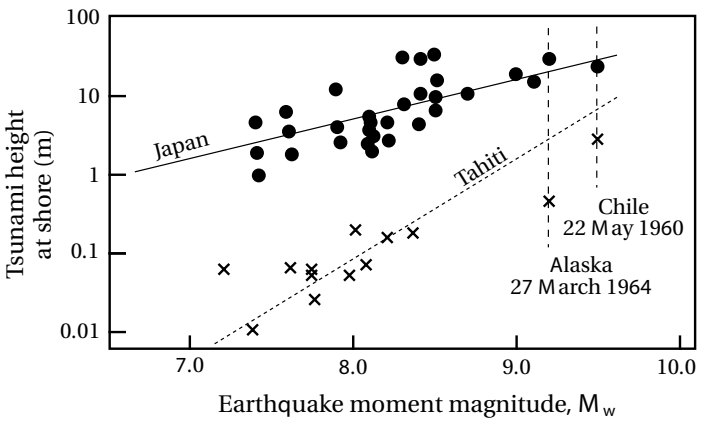

Figure 5.5. Relationship between the moment magnitude, M_w, and tsunami wave height for the east coast of Japan and Tahiti. Based on Okal (1988), and Kajiura (1983).

relationships, respectively:

$$\text{Japan:} \quad \log_{10} \bar{H}_{t\max} = 0.5M_w - 3.3 \tag{5.9}$$

$$\text{Tahiti:} \quad \log_{10} \bar{H}_{t\max} = 1.3M_w - 11.5 \tag{5.10}$$

where $\bar{H}_{t\max}$ = mean maximum tsunami wave height (m) along a coast

The Japanese pattern characterizes dispersive tsunami propagating from point-like sources. Figure 5.5 indicates that tsunamigenic earthquakes generate tsunami that have less of an effect on Tahiti than they do on the east coast of Japan. The reason for this has already been discussed in Chapter 2.

LARGE HISTORICAL TSUNAMIGENIC EARTHQUAKES

Lisbon, November 1, 1755

(Reid, 1914; Myles, 1985; Foster *et al.*, 1991; Andrade, 1992; Moreira, 1993; Dawson *et al.*, 1995; Baptista *et al.*, 1996; Hindson, Andrade, and Dawson, 1996; Whelan and Kelletat, 2005; Scheffers and Kelletat, 2005)

At 9:40 AM on November 1, 1755, All Saints' Day, one of the largest earthquakes ever documented devastated southern Portugal and northwest Africa. Backward ray-tracing simulations, using the type of incompressible, shallow-water long-wave equations outlined in Chapter 2, position the epicenter on the continental shelf less than 100 km southwest of Lisbon (Figure 5.6). This location lies close to the boundary of the

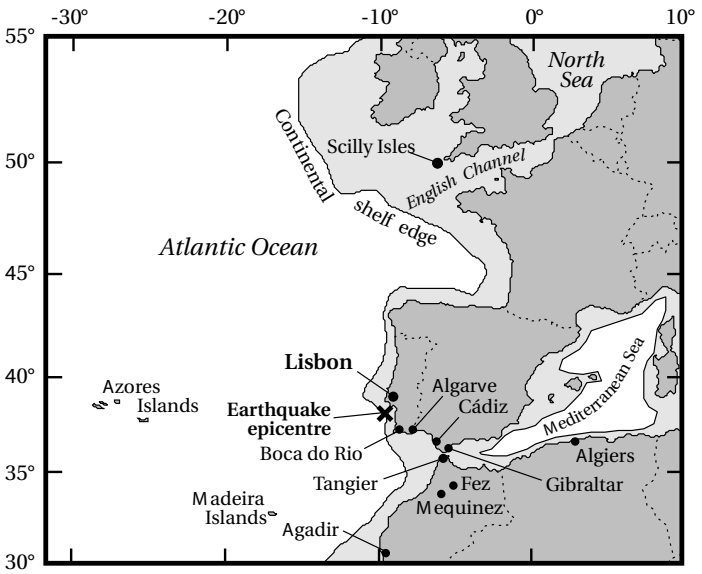

Figure 5.6. Location map for the Lisbon tsunami event of November 1, 1755.

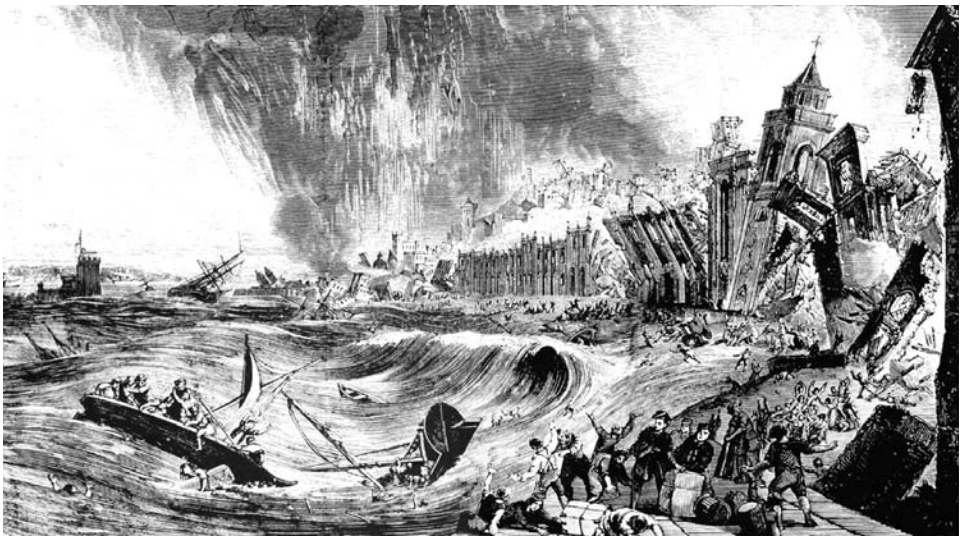

Figure 5.7. Wood engraving by Justine of the tsunami sweeping up the North Tagus River, Lisbon, following the November 1, 1755 earthquake. Note that the earthquake, subsequent fires, and tsunami have been incorrectly drawn as occurring at the same time. *Source:* Mary Evans Picture Library Image No. 10047779/07.

Azores–Gibraltar Plate, which historically has given rise to many tsunamigenic earthquakes in the region. Tsunami have been generated beforehand in this region in 218 BC/216 BC, 210 BC, 209 BC, 60 BC, AD 382, AD 881, AD 1531, AD 1731. The earthquake had an estimated surface wave magnitude, M_s, of 9.0, lasted for 10 minutes, and consisted of three severe jolts. The earthquakes may have generated submarine landslides that contributed to the subsequent tsunami. Heavy loss of life resulted in Lisbon and the Moroccan towns of Fez and Mequinez. Seismic waves were felt throughout western Europe over an area of $2.5 \times 10^6\,\text{km}^2$. Seiching occurred in ponds, canals, and lakes as far north as Scotland, Sweden, and Finland.

Lisbon, a city of 275,000 inhabitants situated 13 km upstream on the Tagus River, was heavily damaged by the earthquake, and consumed by fires. As the fires spread throughout the city, survivors moved down to the city's docks. Some even boarded boats moored in the Tagus River. Between 40 and 60 minutes after the earthquake, the water withdrew from the harbor, and a few minutes later one of the most devastating tsunami in history occurred as a 15 m high wall of water swept up the river, over the docks, and into the city (Figure 5.7). Just as violently, the backwash dragged bodies and debris back out into the estuary. Two other waves subsequently rolled into the city an hour apart.

The tsunami also caused widespread destruction along the coastline of Portugal, where it swept inland up to 2.5 km. At Porto Novo, north of Lisbon, run-up was 20 m high, while at Alvor and Sagres on the southwest tip of Portugal it reached 30 m above sea level. The wave had its greatest impact in southern Portugal. Coastal

fortresses were destroyed, towns flooded, and in the city of Lagos, the city walls lying 11 m above sea level were overtopped. The tsunami also caused widespread devastation in southwest Spain and western Morocco, as well as crossing the Atlantic Ocean and sweeping islands in the Caribbean 5,700 km away. In southwest Spain, the tsunami caused damage to Cádiz and Huelva, and traveled up the Guadalquivir River as far as Seville. At Cádiz, the wave had a run-up of 11 m–20 m. At Gibraltar, the sea rose suddenly by about 2 m; however, the wave's height rapidly decreased as it traveled into the Mediterranean Sea. The Moroccan coast from Tangier to Agadir was severely affected, and in the latter city, the waves swept over the walls of the town, killing many people. The tsunami wave also swept up the west coast of Europe into the North Sea, where it caused great disturbance to local shipping as boats in harbors were pulled from their moorings. Waves 3 m–4 m high moved through the English Channel on a high tide at about 2 AM. The third and fourth waves were the largest. Oscillations in sea level with periods ranging from 10 to 20 minutes occurred over the next 5 hours in places. At Plymouth, the tsunami tore up muds and sandbanks at an alarming rate. The tsunami moved across the Atlantic, damaging the coastline of the Madeira and Azores Islands where wave heights of 15 m were reported. It reached the Caribbean Sea in the afternoon. Reports from Antigua, Martinique, and Barbados noted that the sea first rose more than a meter about 3:30 AM, followed by the arrival of large waves. Run-up heights of 7 m and 4.5 m were observed on the islands of Saba and St. Martin, respectively. On the Leeward Island, Dutch colonists reported waves of 6.0 m–7.5 m in height. Run-ups of 3.0 m–4.0 m were typically observed elsewhere in the eastern Caribbean. Significant oscillations continued at 5-minute intervals over the next 3 hours. In total, about 20,000 people may have been killed by the tsunami, although it is difficult to separate these deaths from those killed by the actual earthquake.

One of the clearest signatures of the Lisbon tsunami was the overwashing of barriers and transport of sands inland over peats. This evidence is clearest along the Algarve coastline of southern Portugal (Figure 5.6), where the tsunami reached its maximum height. The tsunami arrived on a low tide. It was followed by up to 18 secondary waves. At least four other tsunami subsequently affected the same coast between 1755 and 1769. Their impacts form the basis for the model of a tsunami effect on barrier coasts presented in the previous chapter (Figure 4.3). All five tsunami created extensive overwash deposits, infilled lagoons, and led to the creation of a backbarrier flat up to 800 m wide lying 4.0 m–4.5 m above high tide. A narrow foredune ridge now fronts this flat seaward. The flats today are poorly vegetated, with hummocky topography that traces out a labyrinth of second-order drainage channels developed in response to tidal flooding through numerous inlets punched through the barrier by the tsunami. A lag of iron-stained gravels was left on the channel surfaces. The channels merge into first-order meandering ones that are incised progressively seaward into the backbarrier at the location of tidal inlets. The latter formed either major conduits for backwash or short-lived tidal inlets as the barriers recovered. Despite a tidal range of almost 4 m, most tidal inlets closed because the available tidal prism was insufficient to maintain strong enough currents to flush out sediment. Remnant channels are today truncated seaward by a foredune

that has developed in the past 200 years. Some tidal inlets developed wide, flood-tidal deltas in the lagoon. These underwent extensive reworking as tidal currents moved the excessive amounts of sediment. These deltas now lie abandoned in the lagoon.

Along the south Portuguese coast, the tsunami wave also ran up valleys. At Boca do Rio, the tsunami laid down a dump deposit and a tapering sand layer. The dump layer was deposited within 400 m of the coast by the first wave in the tsunami wave train. It consists of a chaotic mixture of muddy sand, cobbles, shell, sand-armored mud balls, and the odd boulder up to 40 cm in diameter. The shells incorporate the littoral bivalve *Petricola lithophaga* and the subtidal sponge *Cliona* spp. The overlying sand layer was laid down by subsequent waves. It consists of a 0.1 m to 0.4 m thick unit sandwiched between silty clays. The unit tapers landward over a distance of 1 km. The sand size within the layer fines upward from a coarse, gritty sand to a silty or clayey, fine sand. The sequence is indicative of high-energy flow that decreased landward. The layer also contains clay 3 μm–12 μm in size that originated from the weathered substratum that was eroded by the passage of the tsunami. Estuarine and intertidal shell species such as *Mytilus edulis*, *Scrobicularia plana*, and *Tellina tenius* are present in the lower part of the layer together with gravels and mud balls 0.5 cm–5.0 cm in size. Foraminifera such as *Elphidium crispum* and *Quinqueloculina seminulum*, both of which are found in 20 m to 30 m depths of water, are present throughout the unit. Dating of the sands indicates that they were deposited by the Lisbon tsunami. However, two previous events around 2,440 yr ± 50 yr and 6,000 yr–7,000 yr ago cannot be excluded. Platy boulders up to 7 m in length were transported by the tsunami in southern Spain. Theoretical flow depths of 14 m–16 m have been calculated using these boulder dimensions.

Sediment signatures of tsunami were also deposited on the Scilly Isles, 40 km southwest of Lands End, England. Here, shallow lagoons backing windswept dune fields and lying about a meter above the high-tide limit were inundated by tsunami swash. The first wave arrived at high tide and produced a 4.5 m high run-up. The third and fourth waves were the largest. Coarse sandy layers 15 cm–40 cm thick were deposited over sandy peats in three lagoons. Over the last 250 years, peat has subsequently covered these sands. Radiocarbon dating at the bottom of this peat indicates that the sands were deposited around the time of the Lisbon event.

Chile, May 22, 1960

(Wright and Mella, 1963; Myles, 1985; Lockridge, 1985; Lander and Lockridge, 1989; Pickering, Soh, and Taira, 1991; Heinrich, Guibourg, and Roche, 1996; Pararas-Carayannis, 1998a)

The most active area seismically producing tsunami is situated along the eastern edge of the Nazca crustal plate, along the coastline of Chile and Peru. This region has been inundated by destructive tsunami at roughly 30-year intervals in recorded history in 1562, 1570, 1575, 1604, 1657, 1730, 1751, 1819, 1835, 1868, 1877, 1906, 1922, and 1960. The May 22, 1960 event was measured at 630 sites around the Pacific Ocean. It is the most widespread tsunami to affect this basin. It was also responsible for the

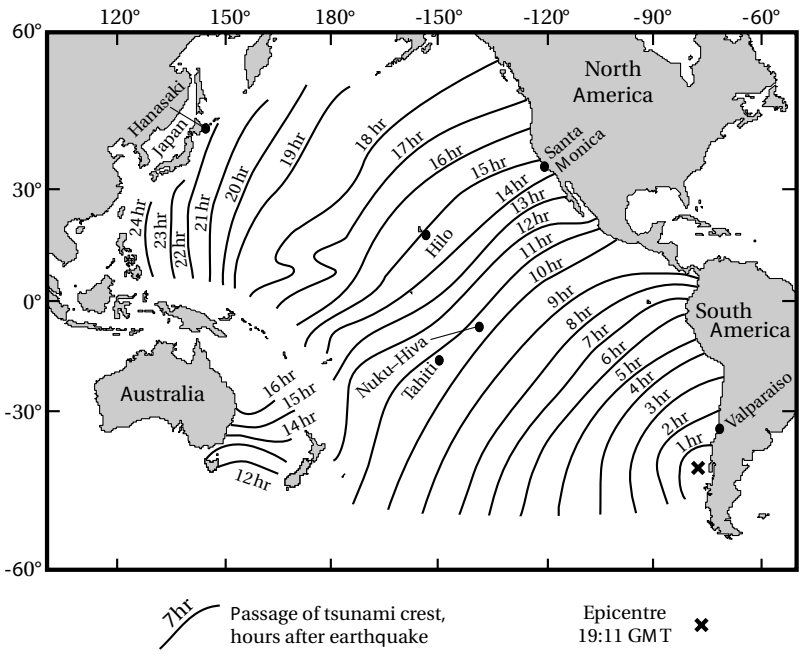

Figure 5.8. Passage of the tsunami wave crest across the Pacific Ocean following the May 22, 1960 Chilean earthquake. Based upon Wiegel (1964), and Pickering, Soh, and Taira (1991).

establishment of the modern Pacific Tsunami Warning System. The May 22, 1960 tsunami was generated by the last of over four dozen earthquakes occurring along 1,000 km of fault line parallel to the Chilean coastline. The first earthquake began at 6:02 AM on Saturday, May 21 and destroyed the area around Concepción. Large aftershocks continued until, at 3:11 PM Sunday, May 22, the largest earthquake with M_s and M_w magnitudes of 8.9 and 9.5, respectively, occurred with an epicenter at 39.5°S, 74.5°W, and a focal depth of 33 km (Figure 5.8). Submarine uplift of 1 m and subsidence of 1.6 m ensued along a 300 km stretch of coast. Subsidence extended as far as 29 km inland with 13,000 km^2 of land sinking by 2 m–4 m. Many fisherman and their families quickly put out to sea to escape the flooding that was to come. Within 10 to 15 minutes, the sea quickly rushed in as a smooth wave 4 m–5 m above normal tide level and just as quickly raced back out to sea taking with it boats and flotsam. This was only the harbinger of worse to come. Fifty minutes later, the sea returned as a thunderous 8 m wall of green water racing at 200 km h^{-1}, drowning all those who had taken to the sea. An hour later, an even higher 11-meter wave came ashore at about half the speed of its predecessor. This was followed by a succession of waves that so obliterated coastal towns between Concepción and the south end of Isla Chiloe that the only evidence left of their existence were the remains of streets (Figure 5.9). Run-up along the Chilean coast near the source area averaged 12.2 m above sea level and ranged between 8.5 m and 25 m (Table 5.4). Dunes were eroded by over-washing, and sand was transported as a thin layer tapering inland over alluvial

Figure 5.9. Aerial view of Isla Chiloe, Chile, showing damage produced by the May 22, 1960 tsunami. Two hundred deaths occurred here. *Source:* National Geophysical Data Center, *http://www.ngdc.noaa.gov/seg/cdroms/Volcanoes/tif_24/648001/64800112.tif*

sediments. In the Valdivia region, 6 cm–30 cm of beach sand was deposited up to 500 m inland, while in the Rio Lingue Valley where the tsunami reached a height of 15 m, a thin layer of sand was deposited up to 6 km inland. The total loss of life in Chile is unknown but probably lies between 5,000 and 10,000. The total property damage from the combined effects of the earthquake and tsunami in Chile was $417 million.

Over the next 24 hours, a series of tsunami wave crests spread across the Pacific, taking 2,231 lives and destroying property in such diverse places as Hawaii, Pitcairn Island, New Guinea, New Zealand, Japan, Okinawa, and the Philippines. The arrival time of the tsunami across the Pacific was accurately measured at many tide gauges (Figure 5.8). The initial wave traveled at a speed of 670 km h^{-1}–740 km h^{-1}, depending upon the depth of the ocean. Individual waves in the tsunami wave train had wavelengths of 500 km–800 km and periods of 40 min–80 min. In the open ocean, the wave height was only 40 cm. Outside of South America, the tsunami reached landfall first along the Mexican, New Zealand, and Australian coasts (Figure 5.8). The tsunami traveled quickest northward along the coast of the Americas across the North Pacific Ocean to Japan. The wave crest underwent refraction around islands in the west Pacific, particularly those in the Izu-Bonin and Marianas Island arcs. Detailed wave refraction analysis indicates that energy was focused toward Japan in the northwest Pacific, but dispersed elsewhere.

Table 5.4. Statistics on the run-up heights of the May 22, 1960 Chilean tsunami around the Pacific Ocean.

Region	*Average height* (m)	*Maximum height* (m)	*Range* (m)
Source area	12.2	25.0	8.5–25.0
Chile	2.7	5.0	0.4– 5.0
Peru	2.0	3.9	1.0– 3.9
Central America	0.5	1.4	0.2– 1.4
U.S. west coast	1.2	3.7	0.2– 3.7
Canada	0.4	0.4	0.1– 0.4
Alaska	1.3	3.3	0.4– 3.3
Hawaii	3.1	10.5	1.5–10.5
Pacific Islands	4.3	12.2	0.5–12.2
Japan	2.7	6.4	0.2– 6.4
New Zealand	0.6	0.9	0.4– 0.9
Australia	0.5	1.8	0.2– 1.8

These effects are reflected in marigrams derived from tidal gauge records around the Pacific Ocean (Figure 5.10). The marigrams show multiple peaks, the highest of which occurred some time after the arrival of the first wave at some locations. Run-ups for the event are summarized by region in Table 5.4. In the southwest Pacific, the tsunami entered the Tasman Sea from the south about 12 hours after the earthquake and caused rapid fluctuations in water levels in many harbors. Run-ups averaged 0.5 m–0.6 m, respectively, along the east coasts of New Zealand and Australia, reaching maximum values of 1.8 m. Boats were torn from their moorings or beached by currents generated by tsunami-induced seiching. Along the coastline of the Americas, where the coast bends eastward, the tsunami had minimal effect with run-ups averaging only 40 cm. On the exposed sections of the west coast of the United States, wave run-up averaged 1.2 m, with values ranging between 0.2 m and 3.7 m. The tsunami also had a variable impact on Pacific Ocean islands. On smaller islands fronted by steep offshore slopes and protecting fringing reefs, waves were only 1 m–2 m in height. However, where gradual bottom slopes existed and bays were present, wave heights were amplified by a factor of 5 and run-ups averaged 4.3 m. Hence, outside the source region, the Pacific Islands were affected the most by the tsunami. For example, on the Marquesas Islands, the wave height of the second wave exceeded

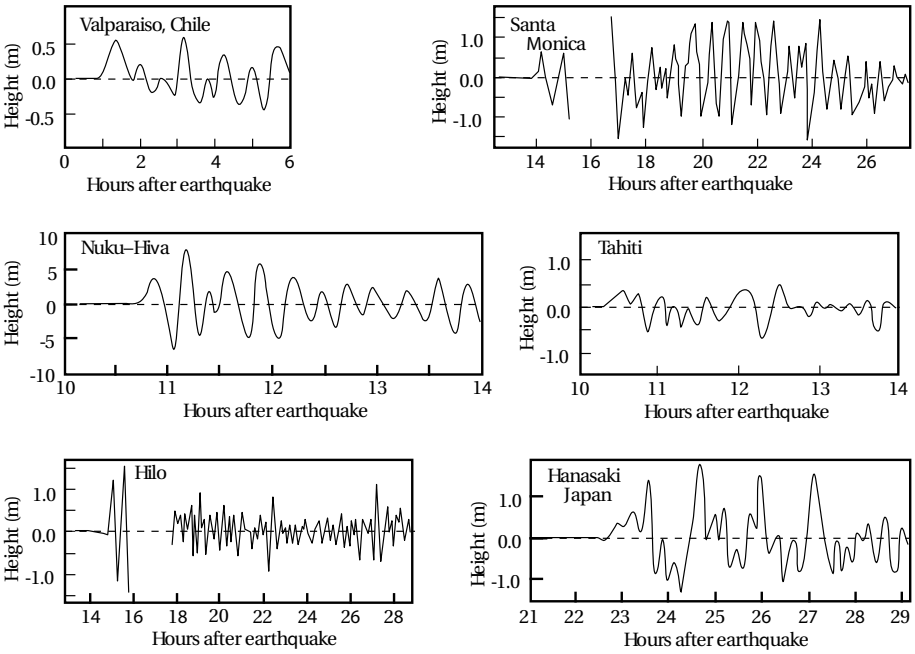

Figure 5.10. Tide records or marigrams of the May 22, 1960 Chilean tsunami around the Pacific Ocean. Records have had their daily tides removed. Based upon Wilson, Webb, and Hendrickson (1962), Tsuji (1991), and Heinrich, Guibourg, and Roche (1996).

10 m at Nuku–Hiva and Hiva–Oa (Figure 5.10). Here, the wave ran up valleys 500 m inland. The largest run-up on any Pacific Island, 12.2 m, occurred on Pitcairn Island.

Hawaii was particularly affected by the tsunami that refracted around to the north side of the island. The greatest impact occurred at Hilo. Here, after traveling 10,000 km over a period of 14.8 hours, the tsunami's arrival time at 9:58 AM was predicted to within a minute. In spite of more than five hours' warning, only 33% of residents in the area affected in Hilo evacuated. Over 50% only evacuated after the first wave arrived, and 15% stayed behind even after the largest waves had beached. The first two waves did not do much damage, but the third wave was deadly. It swept inland 6 m above sea level, reaching a maximum run-up of 10.7 m. Sixty-one people were killed as the wave swept ashore. Many of those killed were spectators who went back to see the action of a tsunami hitting the coast. The waterfront at Hilo was devastated as the waves swept inland over five city blocks (Figure 5.11). Ten-tonne vehicles were swept away and 20-tonne rocks were lifted off the harbor's breakwall and carried inland 180 m. In the area of maximum destruction, only buildings of reinforced concrete or structural steel remained standing. Wooden buildings were either destroyed or floated inland, and piled up at the limit of run-up. About 540 homes and businesses were destroyed or severely damaged. Damage in Hawaii was estimated at $24 million. Subsequently the flooded area was turned into parkland to prevent a recurrence of the disaster.

Figure 5.11. Aftermath of the May 22, 1960 Chilean tsunami in the Waiakea area of Hilo, Hawaii, 10,000 km from the source area. The force of the debris-filled waves bent parking meters. Photograph credit: U.S. Navy. *Source:* National Geophysical Data Center, *http://www.ngdc.noaa.gov/seg/cdroms/Volcanoes/tif_24/648001/64800113.tif*

Although warnings were issued for Japan, the waves struck this country very unexpectedly 22 hours after being generated. The tsunami rose from 40 cm to 70 cm height in 200 m depth of water despite losing 40% of its energy traveling across the Pacific. Dispersion dramatically reduced the height of the initial waves in the tsunami wave train. This effect is shown by the marigram for Hanasaki, Japan, in Figure 5.10. In addition, resonance effects tended to enhance isolated waves in the wave train such that the maximum run-up occurred hours after the arrival of the first waves. Run-up heights averaged 2.7 m along the east coast, with a maximum value of 6.4 m recorded at Rikuzen. At Shiogama and Ofunato on the Sanriku coast of northern Honshu—where local earthquakes, but not distant Pacific ones, had produced such devastating tsunami over the past century—fishing boats were picked up and flung into business districts. Seiching at wave periods much lower than that of the main tsunami occurred in many harbors. Along the shoreline of Hokkaido and Honshu, 5,000 homes were washed away, hundreds of ships were sunk, 251 bridges were destroyed, 190 people

lost their lives, and 854 were injured. Over 50,000 people were left homeless, with property damage estimated at over $400 million.

Alaska, March 27, 1964

(Van Dorn, 1964; Hansen, 1965; Myles, 1985; Lander and Lockridge, 1989; Pararas-Carayannis, 1998b; Johnson, 1999; Sokolowski, 1999a)

The Alaskan earthquake struck on Good Friday, March 27, 1964 at 5:36 PM Alaska Standard Time (03:26 GMT, March 28, 1964) along a seismically active zone paralleling the Aleutian Islands (Figure 5.12a). The area is noted for large tsunamigenic earthquakes that have had a continuing impact upon the Pacific Ocean (Figure 1.2b). Notable events that have affected Hawaii in the previous century occurred on January 20, 1878; April 1, 1946; and March 9, 1957 (Table 1.3). The most recent sequence of seismic activity began in 1938 with large earthquakes in 1938, 1946, 1957, 1964, and 1965. The last three events are amongst the ten largest earthquakes of the 20th century. The southward movement of Alaska over the Pacific Plate at a shallow angle of 20° has generated these earthquakes, forming a subduction zone known as the Aleutian–Alaska Megathrust Zone. Shallow dip favors large trans-Pacific tsunami. The epicenter of the 1964 earthquake was located in northern Prince William Sound at 61.1°N, 147.5°W (Figure 5.12a). The earthquake had a focal depth of 23 km and surface and moment magnitudes of 8.4 and 9.2, respectively—the largest ever measured in North America. The earthquake rang the Earth like a bell and set up seiching in the Great Lakes of North America and in Texas 5,000 km away. Water levels in wells oscillated in South Africa on the other side of the globe. The ground motion was so severe around the epicenter that the tops of trees were snapped off. More significant, ground displacement occurred along 800 km of the Danali Fault system parallel to the Alaskan coastline. The dislocations followed a dipole pattern of positive and negative displacements on either side of a zero line running through the east coast of Kodiak Island, northeast to the western side of Prince William Sound (Figure 5.12b). Maximum subsidence of 3 m occurred west of this line, while as much as 11 m of uplift—the greatest deformation from an earthquake yet measured—occurred to the east. At some locations, individual fault scarps measured 6 m in relief. The earthquake was felt over an area of 1.3×10^6 km^2 while land movement covered an area of 520,000 km^2. Most of Prince William Sound and the continental shelf were affected by the latter deformation. This is the largest area known to be associated with a single earthquake.

Approximately 215,000 km^2 of displacement contributed to the generation of the resulting tsunami over an area measuring 150 km × 700 km. The total volume of crust shifted amounted to 115 km^3–120 km^3. More than 25,000 km^3 of water was displaced. Tsunami generation was also aided by some of the 52 major aftershocks that occurred in the area of uplift. As a result, two main tsunami-generating areas can be distinguished, one along the continental shelf bordering the Gulf of Alaska and the other in Prince William Sound. As the tsunami moved away from the Gulf of Alaska, it was forecast by the Pacific Tsunami Warning System, which had been revamped following the 1960 Chilean tsunami. Within 46 minutes of the earthquake,

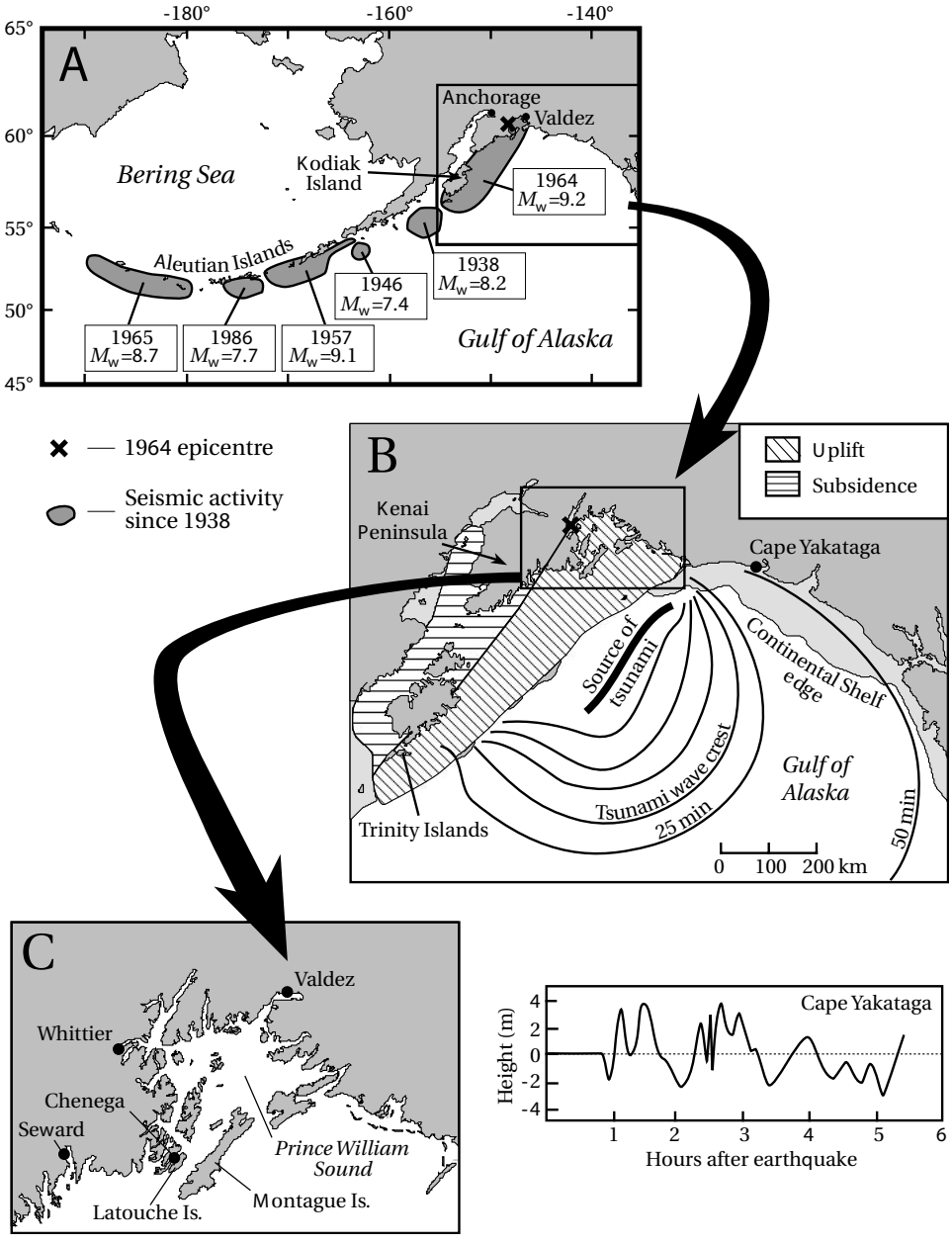

Figure 5.12. Earthquake and tsunami characteristics of the Great Alaskan Earthquake of March 27, 1964. Based on Van Dorn (1965), Pararas-Carayannis (1998b), and Johnson (1999). (A) Location of seismic activity since 1938. (B). Gulf of Alaska land deformation caused by the earthquake and theorized open-Pacific tsunami wave front. (C) Detail of Prince William Sound.

a preliminary, Pacific-wide tsunami warning was issued by the Pacific Tsunami Warning Center in Honolulu. This was not sufficient to warn many Alaskan communities of impending tsunami. For example, the shores of Kenai Peninsula and Kodiak Island were struck by tsunami within 23 and 34 minutes, respectively, of the earthquake. Three major tsunami developed in Prince William Sound. One was related to the earthquake and had its origin near the west coast of Montague Island, at the southern end of the Sound. The second was due to local landslides. The third developed much later in the Port of Valdez region, probably because of resonance within that part of the sound. Maximum positive crustal displacement in Prince William Sound occurred along the northwest coast of Montague Island and in the area immediately offshore. These earth movements caused a gradient in hydrostatic level and numerous large submarine slides in the area off Montague Island and at the north end of Latouche Island. Bathymetric surveys later showed that the combination of submarine slides and the tilting of the ocean floor due to uplift created the solitary wave observed in this region. The tsunami here did not escape the Sound. At Chenega, a solitary wave reached 27.4 m above sea level within 10 minutes of the earthquake.

Landslide-generated tsunami were confined to Prince William Sound where communities generally experienced wave run-ups of 12 m–21 m (Figure 5.12c). At the ports of Seward, Whittier, and Valdez, docks, railway track, and warehouses sank into the sea because of flow failures in marine sediments. The settlements were swamped by 7 m to 10 m high tsunami within an hour of the quake, but local run-ups were greater. None of these communities had any warning of the subsequent tsunami. At Seward, a swathe of the waterfront 100 m wide dropped into the ocean over a distance of 1 km. Twenty minutes later a 9 m high wave rolled into the town picking up the rolling stock of the Alaska Railroad, tossing locomotives like Dinky toys (Figure 5.1), shearing off the pilings supporting the dock, destroying infrastructure and houses, and killing 13 people. Near the harbor, the Texaco oil storage tanks burst and caught fire, spilling flaming oil into the receding sea. An hour later, a second, higher wave roared in. It could not be missed in the dark because it incorporated the flaming oil and raced toward the town as a 10 m high wall of flame. Eerily, the remains of the dock's pilings had caught fire and bobbed like large Roman candles in the waters of Resurrection Bay as successively smaller waves raced in. At Whittier numerous slides occurred. One of the resulting tsunami reached a height of 32 m above sea level. At Valdez, a large submarine slide was generated at the entrance to the port by collapse into the Bay of the terminal moraine at the end of Shoup Glacier. The resulting tsunami lifted driftwood to an elevation of 52 m above sea level and deposited silt and clay 15 m higher. In the town itself, which is situated on an outwash delta with a steep front, an area 180 m wide and 1.2 km long slid into the fjord taking most of the waterfront with it. Within 2 or 3 minutes, a 9 m high wave swept inland through the town (Figure 5.13). Thirty-two people lost their lives, many as the docks collapsed and were then swamped by water. Of the 106 deaths in Alaska due to tsunami related to the Good Friday earthquake, up to 82 were caused by these localized events. About five-to-six hours after the earthquake, further tsunami waves struck Valdez at high tide. The third wave came in at 11 AM March 27, and the fourth

Figure 5.13. Limits of run-up of the tsunami that swept Valdez harbor following the March 27, 1964 Great Alaskan Earthquake. A submarine landslide triggered by the earthquake technically generated this tsunami. The height of run-up was 9 m. Photograph courtesy of the World Data Center A for Solid Earth Geophysics and United States National Geophysical Data Center. *Source:* Catalogue of Disasters # B64C28-205.

one at 1:45 AM March 28. This last wave took the form of a tidal bore and inundated the downtown section of Valdez. Apparently, these last tsunami were produced by resonance that had built up in the Bay over a 5-hour period.

The main tsunami propagated southward into the Pacific Ocean within 25 minutes of the earthquake (Figure 5.12b). Its wave period was exceptionally long, being an hour or more. This was caused by the long seiche period of the shallow shelf in the region where the tsunami originated. At many locations, the first wave arrived as a smooth, rapid rise in sea level rather than as a distinct wave. Seas then receded, to be followed by a bigger wave, often coincident with high tide. On Kodiak Island, the third and fourth waves were the highest and most destructive. Factors such as reflection, wave interaction, refraction, diffraction, and resonance had to be involved in the generation of this tsunami wave train. Kodiak Island sustained heavy damage with a maximum run-up of 10.6 m. The wave was focused south down the west coast of North America. Along the Canadian coast, the wave's height registered about 1.4 m on tide gauges (Table 5.5). However, exposed locations such as Shield Bay recorded a maximum run-up of 9.8 m elevation. The tsunami became the largest historical tsunami disaster to sweep the west coast of the United States. Maximum wave heights reached 4.3 m–4.5 m in all of the three coastal states of Washington, Oregon, and California (Table 5.5). Many seaside towns received only 30 minutes'

Table 5.5. Statistics on the run-up heights of the March 27, 1964 Alaskan tsunami around the Pacific Ocean.

Region	*Average height* (m)	*Maximum height* (m)	*Range* (m)
Source area	11.0	67.0	0.3–67.0
Canada	4.8	9.8	1.4– 9.8
Washington State	1.8	4.5	0.1– 4.5
Oregon	2.8	4.3	0.3– 4.3
California	1.6	4.3	0.3– 4.3
Central America	0.4	2.4	0.1– 2.4
South America	1.2	4.0	0.1– 4.0
Hawaii	2.3	4.9	1.0– 4.9
Pacific Islands	0.2	0.6	0.1– 0.6
Japan	0.4	1.6	0.1– 1.6
Australia–New Zealand	0.2	0.2	—
Palmer Peninsula, Antarctica	0.4	—	—

warning of the wave's arrival. Greatest damage occurred at Crescent City, California, where bottom topography concentrated the wave's energy. Crescent City has been affected by numerous tsunami geologically. Coring of marshes in the area shows evidence for at least 13 previous events, 1 of which laid down a layer of sand 15 cm thick up to 500 m inland. The Alaskan tsunami only laid down a sand layer a centimeter thick in a marsh south of the city. Eleven people were killed in Crescent City by the Alaskan tsunami, most because they returned to low-lying areas before the advent of the fourth and largest wave. As with the Chilean tsunami, dispersion had greatly reduced the height of the first couple of waves in the tsunami wave train. The fourth wave was preceded by a general withdrawal of water that left the inner harbor dry. The wave then rapidly swept ashore, capsizing or beaching fishing boats, destroying piers, and flooding 30 city blocks backing the coast. Up to $8.8 million damage occurred in this one city out of the $12 million damage along the west coast of the United States. Elsewhere the wave swept marinas, tore boats from moorings, and smashed piers. Fortunately, the waves diminished in height significantly before reaching San Francisco, where 10,000 people had flocked to the coast to witness the arrival of this rare event. Farther south at San Diego, authorities were unable to clear sightseers from the beaches.

Following the arrival of the wave in California, warning sirens in Hawaii were sounded to alert the general population to evacuate threatened areas. The first wave arrived at Hilo 1.3 hours after striking Crescent City. Along the exposed shores of Hawaii, run-up averaged 2.3 m high, reaching a maximum of 4.3 m at Waimea on the island of Oahu. Hilo, which had been badly affected by the Chilean tsunami four years beforehand, experienced a run-up of only 3 m in height. Damage here was relatively minor because of the long warning time before the arrival of the waves and because much of the area affected by the Chilean tsunami had not been resettled. Over the next few hours, the wave reached Japan and the South American coasts. In Japan, the effect of the tsunami was minor. The wave averaged 0.4 m high on tide gauges reaching a maximum elevation of 1.6 m (Table 5.5). Little damage was reported. However, the tsunami continued to be a major event along the coast of South America. Here, the wave averaged 1.2 m in height, reaching a maximum value of 4 m at Coquimbo, Chile. Unlike the Chilean event four years previously, individual Pacific islands were not badly affected by the Alaskan tsunami. A maximum wave height of only 0.6 m was registered at the Galapagos Islands. Surprisingly, the Palmer Peninsula in the Antarctic recorded a wave height of 0.4 m—a value greater than that recorded on most Pacific Islands. South Pacific Islands appear to be immune from the effects of tsunami generated by Alaskan earthquakes.

EVENTS OF THE 1990s

(Satake and Imamura, 1995; Schindelé *et al.*, 1995; González, 1999)

In the last decade of the 20th century, there have been 83 tsunami events—a number much higher than the average historical rate of 57 per decade. Like the majority of past events, these tsunami have involved earthquakes and have been concentrated in the Pacific Ocean region (Figure 5.14). The number of deaths during the 1990s has totaled more than 4,000 (Table 5.6). Many of the events were unusual. For example, the October 9, 1995 tsunami in Mexico generated run-up heights of 1 m–5 m elevation. However, in some places the rapidity of inundation was so slow that people could outrun it at a trotting pace. A classic, slow tsunami earthquake caused the Nicaraguan event of September 2, 1992. People at the shore hardly noticed the vibrations, yet within an hour a deadly wave was racing overtop them. One of the most recent tsunami was the Aitape, Papua New Guinea, tsunami of July 17, 1998. It formed the background for one of the stories used in Chapter 1. Again, a tsunami earthquake occurred, with flow depths of over 15 m being recorded. The tsunami that struck the Sea of Marmara, Turkey, on August 17, 1999 was unusual for two reasons. First, it is a good example of a tsunami that was not restricted to an ocean, but that occurred in a small body of water. Second, it was caused by land subsidence because the earthquake occurred on a strike–slip rupture between the Eurasian and Turkish Plates—a feature not conducive to tsunami. Finally, the Vanuatu event of November 26, 1999 brought a slight glimmer of hope that we were getting it correct. The tsunami has not received the publicity of the Flores or PNG events, but on the island of Pentecost, it left a similar scene of destruction. The death toll was only five. People

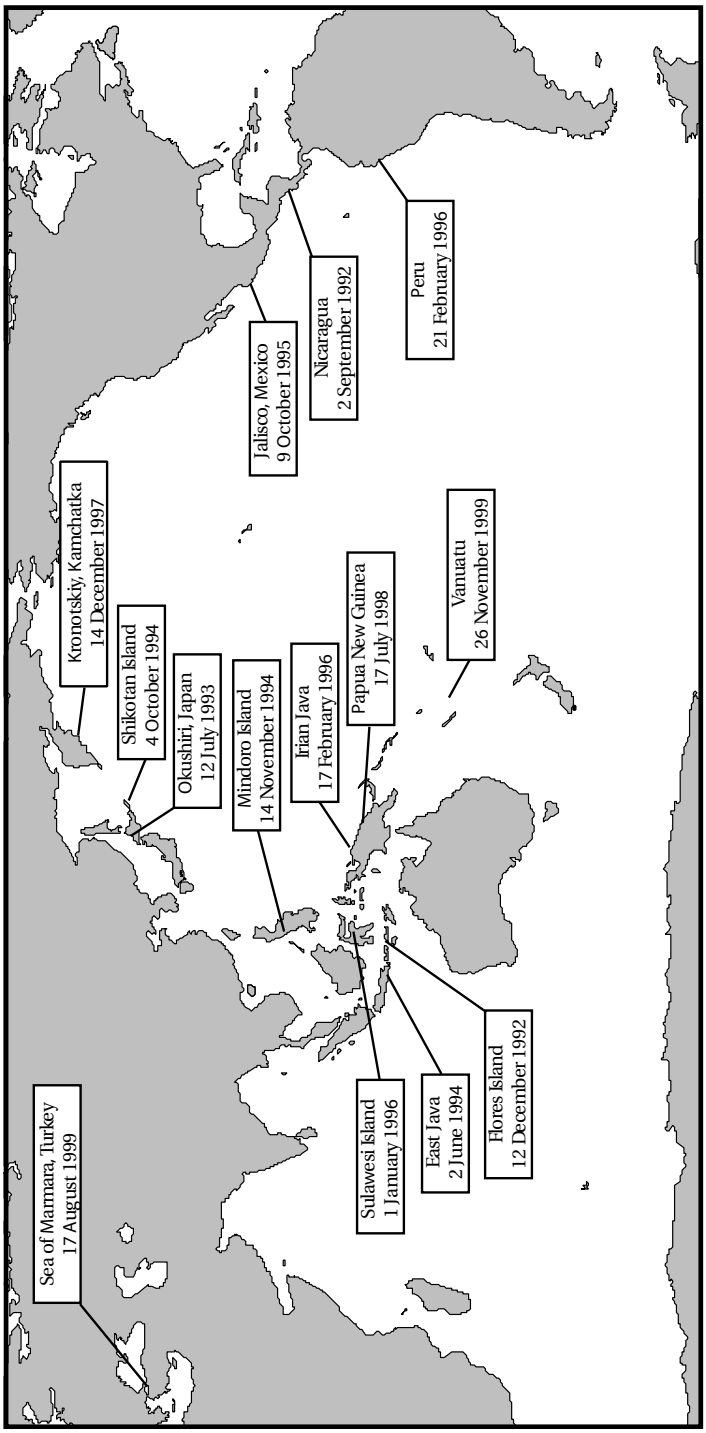

Figure 5.14. Location of significant tsunami during the 1990s.

Table 5.6. Major tsunami of the 1990s.

Location	*Date*	*Earthquake magnitude* (M_s)	*Maximum height* (m)	*Death Toll*
Nicaragua	September 2, 1992	7.2	10.7	170
Flores, Indonesia	December 12, 1992	7.5	26.2	1,713
Okushiri Island, Sea of Japan	July 12, 1993	7.6	31.7	239
East Java	June 2, 1994	7.2	14.0	238
Shikotan, Kuril Islands	October 4, 1994	8.1	10.0	10
Mindoro, Philippines	November 14, 1994	7.1	7.0	71
Jalisco, Mexico	October 9, 1995	7.9	10.9	1
Sulawesi Island, Indonesia	January 1, 1996	7.7	3.4	24
Irian Java	February 17, 1996	8.0	7.7	108
Chimbote, Peru	February 21, 1996	7.5	5.0	2
Kronotskiy Cape, Kamchatka	December 14, 1997	7.7	8.0	—
Aitape, Papua New Guinea	July 17, 1998	7.1	15.0	2,202
Sea of Marmara, Turkey	August 17, 1999	7.8	2.5	?
Pentecost Island, Vanuatu	November 26, 1999	7.3	5.0	5

Source: Based on Satake and Imamura (1995), and Internet sources.

had fled to safety after they noticed a sudden drop in sea level. Though there was little memory of any previous tsunami, they had recently been shown an educational video based upon the PNG event and had reacted accordingly. This section will describe four of these events in Nicaragua, Flores, Japan, and Papua New Guinea.

Slow Nicaraguan tsunami earthquake of September 2, 1992

(Abe *et al.*, 1993; Kanamori and Kikuchi, 1993; Satake *et al.*, 1993; Geist, 1997b)

The Nicaraguan tsunami earthquake occurred at 7:16 PM (00:16 GMT) on September 2, 1992, 70 km offshore from Managua (Figure 5.15). The earthquake had a surface wave magnitude, M_s, of 7.0–7.2 and a moment magnitude, M_w, of 7.7. It had a shallow focal depth of 45 km. Aftershocks occurred along the strike, parallel to the coast of Nicaragua in a band 100 km wide and 200 km long. The rupture occurred as the result of slow thrusting along the shallow-dipping subduction interface between

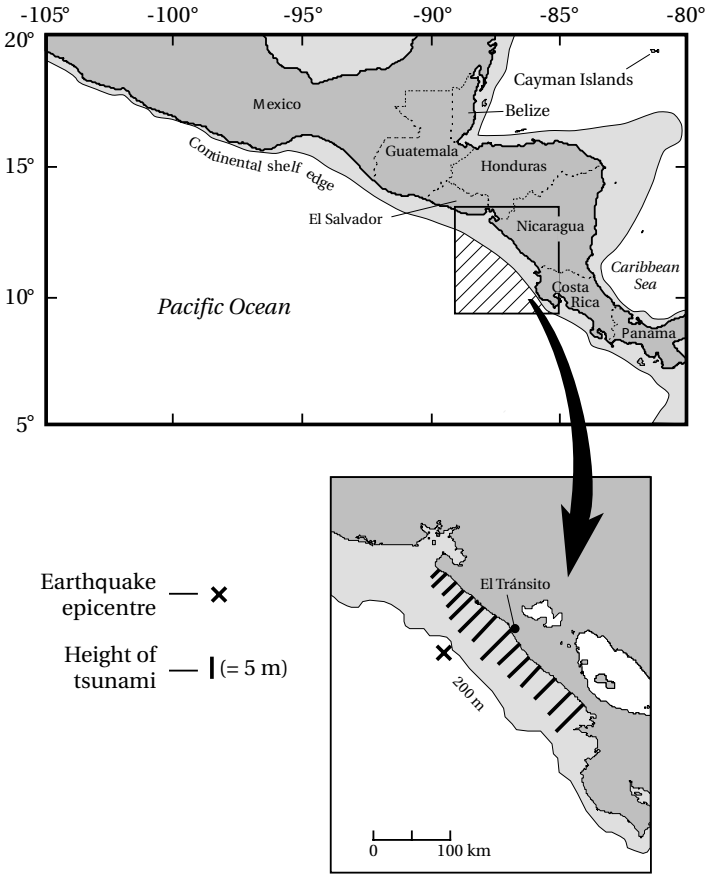

Figure 5.15. Location and height of Nicaragua tsunami of September 2, 1992. Height bars are scaled relative to each other.

the Cocos and Caribbean Plates near a previously identified seismic gap. The rupture propagated smoothly up-dip and alongshore at a velocity of 1.0 km s^{-1}–1.5 km s^{-1} over a period of two minutes (Figure 5.2). For these reasons, the earthquake was barely felt by residents along the coast. The earthquake's moment magnitude, M_w, was 7.7, a value at least half an order of magnitude greater than the surface wave magnitude, M_s, of 7.2—a disparity that characterizes tsunami earthquakes. The tsunami magnitude, M_t, was 7.9–8.0, much higher than should have been generated by an earthquake of this size.

The slow movement of the seabed generated a tsunami that reached the coastline 40–70 minutes later. Healthy adults, who were awake at the time, were able to outrun the tsunami. The tsunami killed 170 people, mostly children who were asleep and infirm people who could not flee. Run-up averaged 4 m along 2 km of coastline (Figure 5.15) and reached a maximum value of 10.7 m near El Tránsito

Figure 5.16. El Tránsito, Nicaragua after the tsunami of September 2, 1992. While the second wave, which was 9 m high at this site, destroyed most of the houses, only 16 out of 1,000 people died because most fled following the arrival of the first wave, which was much smaller. Photo credit: Harry Yeh, University of Washington. *Source:* NOAA National Geophysical Data Center.

(Figure 5.16). This is about ten times higher than the amplitude of a tsunami that should be generated by this size earthquake. Highest run-up appears to correlate with zones of greatest release of seismic force and maximum slip along the fault. Sand was eroded from beaches and transported, together with boulders and building rubble, tens of meters inland (Figure 5.16). The wave also propagated westward into the Pacific Ocean. A 1 m wave was measured on tide gauges on Easter and Galapagos Islands, and a 10 cm wave was measured at Hilo, Hawaii, and Kesen'numa, Japan.

Flores, December 12, 1992

(Yeh *et al.*, 1993; Shi, Dawson, and Smith, 1995; Tsuji *et al.*, 1995; Minoura *et al.*, 1997)

The Flores tsunami occurred at 1:29 PM (05:29 GMT) on December 12, 1992 along the north coast of the island of Flores in the Indonesian Archipelago (Figure 5.17). An earthquake as the result of back-arc thrusting of the Indo-Australian Plate northward beneath the Eurasian Plate generated the tsunami. The earthquake had a surface wave magnitude, M_s, of 7.5. Damaging earthquakes and their tsunami have tended to increase in the Flores–Alor region since 1977, with at least nine earthquakes being reported beforehand. The 1992 earthquake had an epicenter at the coast and produced general subsidence of 0.5 m–1.0 m. Within 2 or 3 minutes a tsunami arrived

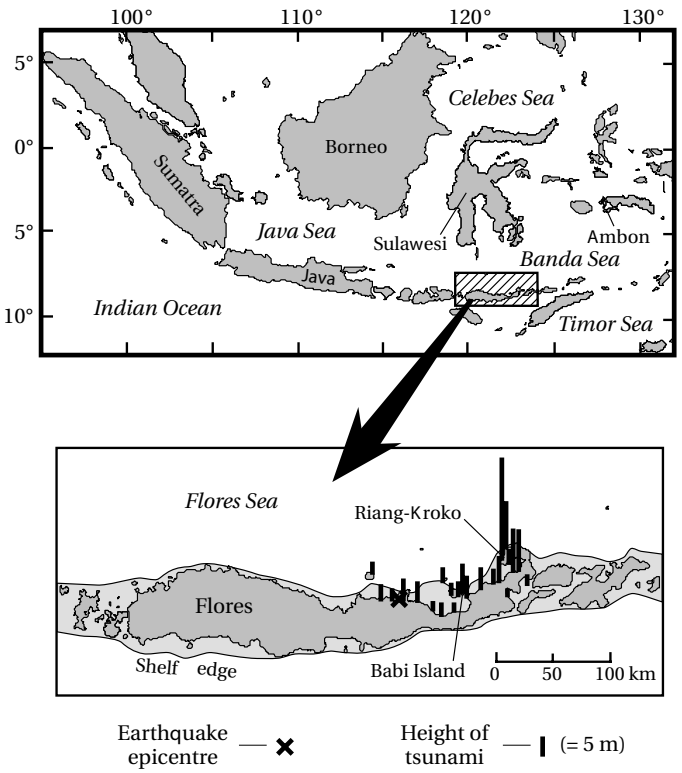

Figure 5.17. Location and height of the Flores, Indonesia tsunami of December 12, 1992. Based on Tsuji *et al.* (1995). Height bars are scaled relative to each other.

ashore to the east, and within 5 minutes the tsunami reached most of the coastline where damage occurred. The tsunami wave train consisted of at least three waves, with the second one often being the largest. The first wave, which came in as a wall, was preceded by a general withdrawal of water. Submarine landslides triggered by the earthquake may explain many of the tsunami's features including the small number of waves in the wave train and the larger run-up heights and shorter arrival times eastward (Figure 5.17). Run-up heights varied from 2 m to 5 m in the central part of the island, to as much as 26.2 m in the village of Riang–Kroko (Figure 3.6), on the northeast tip of Flores, where 137 of the 406 inhabitants were killed. This tsunami is only 1 of 3 that occurred in the 20th century with run-up exceeding more than 20 m. Overall, 2,000 deaths occurred as the waves destroyed entire villages. Damage was especially heavy on Babi Island, which lies 5 km offshore. Here the tsunami refracted around to the landward side of the island and ran up to heights of 7.2 m above sea level on the southwest corner. Of the 1,093 inhabitants on this island, 263 were drowned. The tsunami also affected the southern coast of Sulawesi Island where 22 people were killed. Two hours after the earthquake, smaller waves arrived at Ambon-Baguala Bay on Ambon Island.

Along much of the affected coastline, widespread erosion took place, denoted by coastal retreat, removal of weathered regolith and soils, and gullying. Small cliffs were often created by soil stripping, probably as the result of downward-eroding vortices within turbulent flow. The tsunami spread a tapering wedge of sediment 0.01 m–0.5 m in thickness as much as 500 m from the coast. The wedge consisted of sand material swept from the beaches and shell and coral gravels torn up from the fringing reefs. Clay and silts appear to have been winnowed from the deposits by preceding tsunami backwash. Grain size tended to decrease, but sorting increased, toward the surface of these deposits. This pattern indicates an initial rapid rate of sedimentation. Grain size also tended to fine inland as the competence of the flow decreased concomitantly with a decrease in flow velocity. On Babi Island, there was a coarsening of grain size at the limit of run-up. Saw-tooth changes in grain size upward through the deposits indicate that more than one wave was responsible for laying down the sand sheet. Sediment sequences on Babi Island imply that two different tsunami struck: the first from the direction of the earthquake and the second as the result of a trapped edge wave refracting around the island. This second wave was stronger than the first because it transported coarser material including large mollusks. Modeling indicates that the first wave had a run-up velocity of $1\,m\,s^{-1}$, while the second one traveled faster at velocities of $2\,m\,s^{-1}$–$3\,m\,s^{-1}$.

The Hokkaido Nansei–Oki tsunami of July 12, 1993

(Yanev, 1993; Sato *et al.*, 1995; Oh and Rabinovich, 1994; Shimamoto *et al.*, 1995; Shuto and Matsutomi, 1995)

In the late evening at 11 : 17 PM (13 : 17 GMT) on July 12, 1993 a strong earthquake with a moment magnitude, M_w, of 7.8 was widely felt throughout Hokkaido, northern Honshu, and adjacent islands (Figure 5.18). The earthquake occurred in the Sea of Japan, north of Okushiri Island. The Sea of Japan has historically experienced 20 tsunami, 4 of which have occurred in the 20th century. The 1993 event occurred in a gap between the epicenters of the 1940 and 1983 earthquakes (Figure 5.18), and had a focal depth of about 34 km. This location coincides almost exactly with the epicenter of the Kampo earthquake of August 29, 1741, which produced a tsunami with a maximum run-up of 90 m along the adjacent Japanese coast. Aftershocks from the 1993 event covered an ellipsoid 150 km long and 50 km wide close to Okushiri Island. About 150 km of faulting may have been involved in the event. The earthquake consisted of at least five intense jolts spaced about 10 seconds apart (Figure 5.2). Two to five minutes later a tsunami with an average run-up height of 5 m spread along the coast of Okushiri Island and killed 239 people—many of whom were still trying to flee the coastal area. On the southwestern corner of the island, run-up reached a maximum elevation of 31.7 m in a narrow gully. This is the highest run-up of the century in Japan, surpassing that of the deadly Sanriku tsunami of 1933. Tsunami walls up to 4.5 m high protecting most of the populated areas were over-topped by the tsunami. Similar walls have been constructed in and around Tokyo and other metropolitan areas of Japan to protect urban areas from tsunami. They may be just as ineffective. In the town of Aonae, at the extreme southern tip of Okushiri

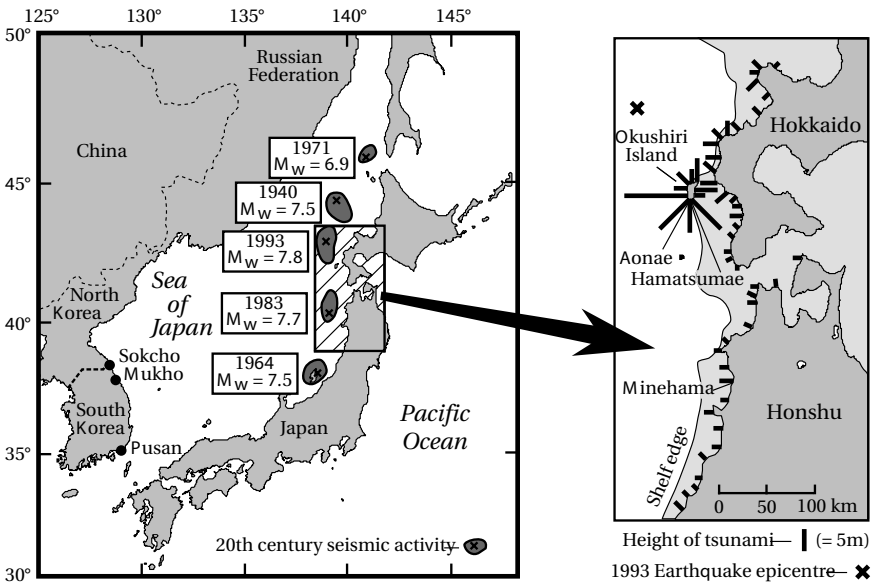

Figure 5.18. Areas and epicenters of 20th century seismic activity in the Sea of Japan. Based on Oh and Rabinovich (1994). Detailed map shows location and height of the Hokkaido Nansei–Oki tsunami of July 12, 1993. Based on Shuto and Matsutomi (1995). Height bars are scaled relative to each other.

Island, the first wave arrived from the west with a height of 7 m–10 m, overtopping the protective barriers and destroying the exposed southern section of the town (Figure 5.19). About 10 to 15 minutes later a second tsunami struck the sheltered, unprotected, eastern section of the town from the east, igniting fires that burnt most of the remaining buildings. The possibility that the second wave originated from aftershocks cannot be ruled out. The tsunami washed away half of the 690 houses in the town, although most were bolted to concrete foundations. The tsunami also severely damaged port facilities, power lines, and roads, stripping away pavement and depositing it inland. At Hamatsumae, which lies in the sheltered southeast corner of the island, run-up measured 20 m above sea level. This high run-up was most likely due to refraction of a trapped soliton around the island—an effect similar to that produced around Babi Island during the Flores tsunami.

Within 5 minutes of the earthquake, the tsunami also struck the west coast of Hokkaido with a maximum run-up of 7 m elevation. The simultaneous arrival times along Hokkaido and Okushiri Islands suggests that there may have been another tsunamigenic mechanism involved in generating the tsunami. Tsunami run-up decreased on the north coast of Honshu; however, southward, it reached a height of 3.5 m at Minehama. Fifty to 70 minutes after the earthquake, the tsunami reached the coastline on the opposite side of the Sea of Japan, striking the Russian coast with an average run-up of 2 m–4 m elevation. Forty minutes after this, the wave reached the South Korean coast at Sokcho and propagated southward to Pusan over the next

Figure 5.19. Damage at Aonae, Okushiri Island, due to the Hokkaido Nansei–Oki tsunami of July 12, 1993. The earthquake, and not the tsunami, damaged the leaning lighthouse. Concrete foundations in the foreground have been wiped clear of shops, houses, and kiosks. Note the gravel and boulder dump deposit, and the similarity of the unit to that deposited by the Flores tsunami in Figure 3.6. Photo credit: Dennis J. Sigrist, International Tsunami Information Center at Honolulu, Hawaii. *Source:* National Geophysical Data Center.

ninety minutes. The tsunami wave height, as measured on tide gauges, was 0.2 m, 1.8 m, and 2.7 m, respectively, at Pusan, Sokcho, and Mukho. At Sokcho and Mukho, where the coastline and continental shelf edge are smooth and straight, waves were detectable for the next two days with periods averaging around 10 minutes. Along the Pusan coast, dominated by bays and islands, wave periods were two to three times longer and decayed more slowly. It appears that tsunami amplification took place along the central Korean Peninsula, while seiching occurred along the south coast in bays and harbors. There was also evidence of resonance effects in the Sea of Japan as a whole.

The tsunami's characteristics were heavily dependent upon the configuration of the coastline. At some locations sea level withdrew before the arrival of the tsunami crest, while at others the crest arrived first. Equal numbers of localities reported either the first or the second wave as the biggest. Run-up heights in many locations were two to three times greater than the initial height of the wave at shore. Calculations of the force required to remove houses bolted to concrete slabs indicate that flow velocities reached maximum values of between $10\,m\,s^{-1}$ and $18\,m\,s^{-1}$. The tsunami deposited 10-cm thick sandy splays behind sand dunes. At Aonae, dump deposits several tens of

centimeters thick were observed around obstacles and a sheet of poorly sorted sediment and debris was deposited throughout the village (Figure 5.19). This material rarely was transported inland more than 200 m. Internal, seaward-dipping bedding in some deposits indicates that upper flow regime antidunes formed. Where it first made landfall, the second tsunami cut parallel grooves up to 40 cm deep across the foreshore. Erosion also occurred with the formation of turbulent vortices around obstacles and in channelized backwash. Flow velocities interpreted from these sediment features agree with those interpreted from structural damage to buildings.

Papua New Guinea, July 17, 1998

(Gelfenbaum and Jaffe, 1998; Hovland, 1999; Kawata *et al.*, 1999; Tappin *et al.*, 2001)

Historically, the Sissano coast of northwest Papua New Guinea (PNG) has been no more at risk from tsunami than any other South Pacific island in a zone of known seismic activity. Two previous earthquakes in 1907 and 1934—neither of which seems to have generated a tsunami of any note—appear responsible for the formation of Sissano lagoon. Tsunami have occurred in the past, because a thin buried sand layer sandwiched within muds exists in the Arop area. At 6:49 PM (08:49 GMT) on July 1998, an earthquake with an M_s magnitude of 7.1 shook this coast. Twenty minutes later a moderate aftershock with a moment magnitude, M_w, of 5.75 jolted the coastline. Later analysis indicates that this second event was preceded by 30 seconds of slow ground disturbance. The location of the epicenter is still indeterminate; but the spread of aftershocks indicates that the earthquake was most likely centered offshore of Sissano lagoon, on the inner wall of the New Guinea trench that forms a convergent subduction zone where the Australian Plate is overriding the north Bismarck Sea. The Pacific Tsunami Warning Center detected the first earthquake and issued an innocuous tsunami information message about an hour later (Figure 5.20). In the meantime, a devastating tsunami with a tsunami magnitude, M_t, of 7.5 had already inundated the Sissano coastline shortly after the main aftershock. Tsunami flow depth averaged 10 m deep along 25 km of coastline (Figure 5.21), reaching a maximum 17.5 m elevation. The wave penetrated 4 km inland in low-lying areas. In places, the inundation of water was still 1 m–3 m deep 500 m inland. The wave also was measured at Wutung on the Indonesian border, where it reached a height of 2 m–3 m. It then propagated northward to Japan and Hawaii where 10 cm to 20 cm oscillations were observed on tide gauges about seven hours later. Over 2,200 people lost their lives.

The wave was unusual because it was associated with fire, bubbling water, foul-smelling air, and burning of bodies. Eyewitnesses reported that the crest of the tsunami was like a wall of fire with sparkles flying off it. In Chapter 1, this sparkling was attributed to bioluminescence, while the foul odor was linked to disturbance of methane-rich sediments in Sissano lagoon. The burnt bodies have been ascribed to friction as people were dragged hundreds of meters by the wave through debris and trees. These explanations may not be correct. Subduction zones incorporate organic material, which is converted to methane by anaerobic decomposition. The sudden withdrawal of 1 m–2 m depth of water can cause degassing of these sediments, leading

Subject: Tsunami Information Bulletin
Date: Fri, 17 Jul 1998 09:46:05 GMT
From: TWS Operations <ptwc@PTWC.NOAA.GOV>
To: TSUNAMI@ITIC.NOAA.GOVTSUNAMI

BULLETIN NO. 001
PACIFIC TSUNAMI WARNING CENTER/NOAA/NWS
ISSUED AT 0943Z 17 JUL 1998

THIS BULLETIN IS FOR ALL AREAS OF THE PACIFIC BASIN EXCEPT CALIFORNIA, OREGON, WASHINGTON, BRITISH COLUMBIA, AND ALASKA.

. . THIS IS A TSUNAMI INFORMATION MESSAGE, NO ACTION REQUIRED . .

AN EARTHQUAKE, PRELIMINARY MAGNITUDE 7.1 OCCURRED AT 0850 UTC 17 JUL 1998, LOCATED NEAR LATITUDE 2S LONGITUDE 142E
IN THE VICINITY OF NORTH OF NEW GUINEA

EVALUATION: NO DESTRUCTIVE PACIFIC-WIDE TSUNAMI THREAT EXISTS. HOWEVER, SOME AREAS MAY EXPERIENCE SMALL SEA LEVEL CHANGES.

THIS WILL BE THE ONLY BULLETIN ISSUED UNLESS ADDITIONAL INFORMATION BECOMES AVAILABLE.

. . . NO PACIFIC-WIDE TSUNAMI WARNING IS IN EFFECT . . .

Figure 5.20. Message issued by the Pacific Tsunami Warning Center following the Papua New Guinea earthquake of July 17, 1998.

to bubbling water. The tsunami crest approached the coastline at 100 km h^{-1}. The atmospheric pressure pulse preceding this wave may have been sufficient to ignite this methane. Certainly, the pulse was strong enough to flatten people to the ground before the wave arrived. Those exposed to this flaming wall of water would have been severely burnt before being carried inland.

The wave also deposited one of the classic sedimentary signatures of tsunami by moving a million cubic meters of sand onshore and spreading it as a 5 cm to 15 cm thick splay inland along the coast. At Arop, the sand deposit was up to 2 m thick and reached 60 m–675 m inland (Figure 5.22). The basal contact of the deposit was erosional. Mud rip-up clasts were evident in places, indicating high-velocity turbulent flow. Grain size decreased both upward throughout the deposit and landward—facts reflecting the reduced capacity of the flow to carry sediment with time. Theory indicates that a 7.1-magnitude earthquake could not have produced a tsunami higher than 2 m along this coastline. While the event would appear to be a tsunami earthquake, its moment magnitude, M_w, was also too low, having a value of 7.1—far less

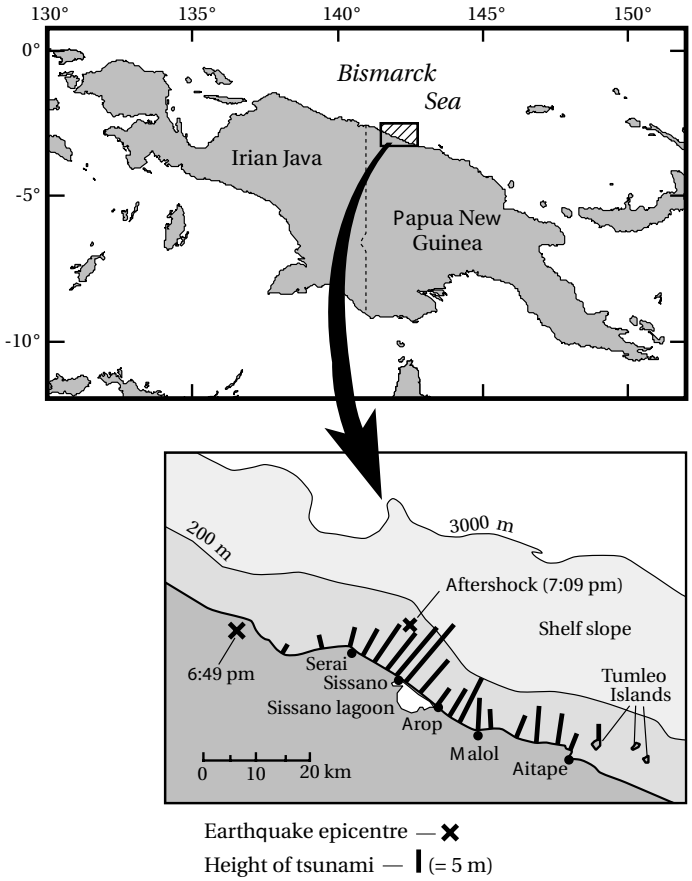

Figure 5.21. Location and height of Aitape, Papua New Guinea tsunami of July 17, 1998. Based on Kawata *et al.* (1999), and Tappin *et al.* (1999). Height bars are scaled relative to each other.

than that generated by tsunami earthquakes. Submarine landslides have been suggested as a cause for large tsunami following small tsunamigenic earthquakes. This now appears to be the main cause of this tragic event, and is supported by the fact that there were only three closely spaced waves in the tsunami wave train. Sea level withdrew from the coast, although there is evidence that about 0.4 m of submergence took place at the coastline. This pattern is similar to, though more rapid than, that of the 1960 Chilean tsunami along the Concepción coast. Eastward the wave did not approach shore-normal but traveled at an angle to the shore. This is unusual for seismically generated waves originating beyond the continental shelf but fits dispersion away from the point source of a submarine slump. Offshore mapping has now delineated slump scars, fissures, and amphitheatre structures associated with rotational slides. Given the closeness of the epicenter to shore, the tsunami should have

Figure 5.22. Overwash splay of sediment caused by the July 17, 1998 tsunami at Arop, Papua New Guinea. The splay is up to 2 m thick. Note the number of trees left standing despite the tsunami being over 15 m high and traveling at a velocity of 15 m s^{-1}–20 m s^{-1} near the shoreline. *Source:* Dr. Bruce Jaffe and Dr. Guy Gelfenbaum, U.S. Geological Survey.

arrived within 10 minutes of the earthquake. It took 10 minutes longer. Slumping takes time after an earthquake to generate a tsunami, and this fact can account for the delay. If a submarine landslide generated the tsunami, theoretically 5 km^3 of material would have had to be involved. Alternatively, numerous slides could have coalesced instantaneously over an area of 1,000 km^2. The most recent evidence indicates that a slump with a volume of 6 km^3 triggered the tsunami. Topographic focusing must have occurred to produce the tsunami flow depths measured along the Aitape coast.

The Papua New Guinea event raises a conundrum in ascribing tsunami to the occurrence of an antecedent earthquake no matter what its size. Secondary landslides were associated with many of the events described in this chapter. For example, many of the tsunami in Prince William Sound following the Alaskan earthquake were due to localized submarine landslides. At present, slides are perceived only as a minor

contributor to tsunami. This view may be neglectful given the fact that many tsunamigenic earthquakes occur along the slopes of steep continental shelves prone to topographic instability. For example, the Tokyo earthquake of September 1, 1923 caused the seafloor to drop in elevation by 400 m in places. Under the circumstances, it has been difficult to resolve what process generated the PNG tsunami, which reached run-ups of over 15 m near Sissano lagoon (Figure 5.21). A submarine slump has now emerged as the most likely candidate. This underrated aspect of tsunami will be discussed in depth in the next chapter.

THE INDIAN OCEAN TSUNAMI, DECEMBER 26, 2004

(Ammon *et al.*, 2005; Bilham, 2005; Kawata *et al.*, 2005; Lay *et al.*, 2005; Titov *et al.*, 2005; Choi, Hong, and Pelinovsky, 2006; Nagarajan *et al.*, 2006; National Oceanic and Atmospheric Administration, 2006; Subarya *et al.*, 2006; Paris *et al.*, 2007)

The Indo-Australian Plate is moving northward against the southern extension of the Eurasian Plate at the rate of 37 mm yr^{-1}–57 mm yr^{-1}. However, no large earthquake with a moment magnitude, M_w, greater than 8.0 had occurred along the boundary of these two plates for over a century. Severe earthquakes had occurred in the region previously in 1797 ($M_w = 8.2$), 1833 ($M_w = 9.0$), 1861 ($M_w = 8.5$), and 1881 ($M_w = 7.9$) with some producing destructive local tsunami. However, for over a century, the region was relatively quiescent seismically. On December 23, 2004 at 14:59.03 UTC the whole Australian plate began to move starting with a magnitude 8.1 earthquake north of Macquarie Island 900 km southeast of Australia. Late Christmas Day, Greenwich Mean Time, an experimental seismometer located at the University of Wollongong, south of Sydney, Australia, measured the passage of a very long wave moving northward through the Earth's crust. The Australian Plate was flexing. Two hours later, at 58 minutes and 47 seconds past midnight Greenwich Mean Time, 7:58.47 AM local time at Jakarta, on the December 26, 2004 (Boxing Day) the enormous pressures that had built up over the past century began to rupture the plate boundary 30 km below sea level at 3.3°N, 95.9°E, about 160 km offshore of northern Sumatra. For 10 minutes, the Indo-Australian Plate moved northward slowly at first and then accelerating to a speed of 2.8 km s^{-1} over a distance of 1,200 km–1,300 km. As the plates unzipped, the Eurasian Plate jumped to the southwest. Between the Andaman Islands and Nias Island, slip displacements reached 15 m over a 600 m length of the plate boundary centered on Banda Aceh, Indonesia. The size of the earthquake defied analysis for months because so much energy was concentrated in long seismic waves. In the end, the moment magnitude, M_w, was estimated at between 9.15 and 9.30, equivalent to 1.1×10^{18} J, more that the total energy released by all earthquakes globally over the previous ten years. The number of aftershocks greater than 5 in magnitude was the greatest ever observed. The earthquake was felt as far north as Bangladesh and as far west as the Maldives. The whole surface of the earth moved vertically at least one centimeter. The shift in

mass slowed the Earth's rotation by 2.7 microseconds. It was the second largest earthquake ever recorded.

Vertical, upward displacement of the seafloor off Sumatra reached 1 m–2 m and the ocean above heaved in response, displacing 30 km^3 of seawater that then propagated outward along the 1,200 km distance of the fault line. A disaster of global proportions was unwinding as the deadliest tsunami in recorded history began to race across the Andaman Sea and the Indian Ocean. The event is definitive: it was the most devastating Sunday morning in human history, the deadliest tsunami ever, and for the Indian Ocean very unexpected. There was also one major difference between large tsunami in the Indian Ocean over a century ago and now. The increased population that had spread onto coastal plains in Sumatra, Sri Lanka, India, and Thailand since the Second World War were all vulnerable. There was no warning for the thousands who would die over the next 10 hours, for the Indian Ocean had no tsunami warning capability. Nor would a warning system have been that effective because 73% of the death toll occurred within 20–30 minutes of the earthquake. At Banda Aceh on the northern tip of Sumatra, the sea receded 10 minutes after the earthquake. Three minutes later the first wave measuring 5 m in height ran ashore. Five minutes after this a second and more devastating wave arrived with heights of 15 m–30 m. Very few observations exist of the third and final wave, because most people were dead.

The tsunami as it spread outward throughout the Indian Ocean had a height of 60 cm, exceeding the height of the Chilean tsunami described previously. For the first time, this height could be measured using altimeters on satellites: TOPEX/Poseidon and Jason operated jointly by NASA and the French space agency (Figure 5.23c), CNES, the European Space Agency's Envisat, and the U.S. Navy's Geosat Follow-On, that fortuitously passed above the wave front in the region of Sri Lanka. The measurements backed up theory indicating that the tsunami in 4,500 m depths at the time of sensing had a shallow-water wave speed of about 750 $km\,h^{-1}$. The period of the wave, after correcting for the speed of the satellite, was about 37 minutes. The wave took 10 hours to cross the Indian Ocean. The height of the tsunami on local tide gauges is difficult to ascertain because many were destroyed. No records exist in northern Sumatra. At Phuket, Thailand, a depth sounder located 1.6 km offshore recorded the passage of a 6 m high wave. However, closer to the coast, this wave did not appear to be more than 3.2 m high (Table 5.7). Along the east coast of India, the wave had a maximum inshore height—measured from the trough to the wave crest—of 3.2 m. In Sri Lanka, the wave at Colombo on the sheltered west coast, measured only 2.2 m in amplitude. It was certainly higher than this on the exposed east coast, but no tide gauge recorded its passage.

The tsunami became only one of three—Krakatau in 1883 and the Chilean tsunami of 1960 described above were the other two—to propagate into other oceans. It was measured on almost every tide gauge globally. Surprisingly, mid-ocean ridges acted as waveguides beaming tsunami wave energy into other oceans and giving rise to some unexpected heights on distant shores on the other side of the globe. For example, the tsunami reached Rio de Janeiro, Brazil and Halifax, Canada where heights of 100 cm and 43 cm, respectively, were recorded (Table 5.7). The tsunami had to travel 24,000 km to reach Halifax. The energy was transmitted to these sites around

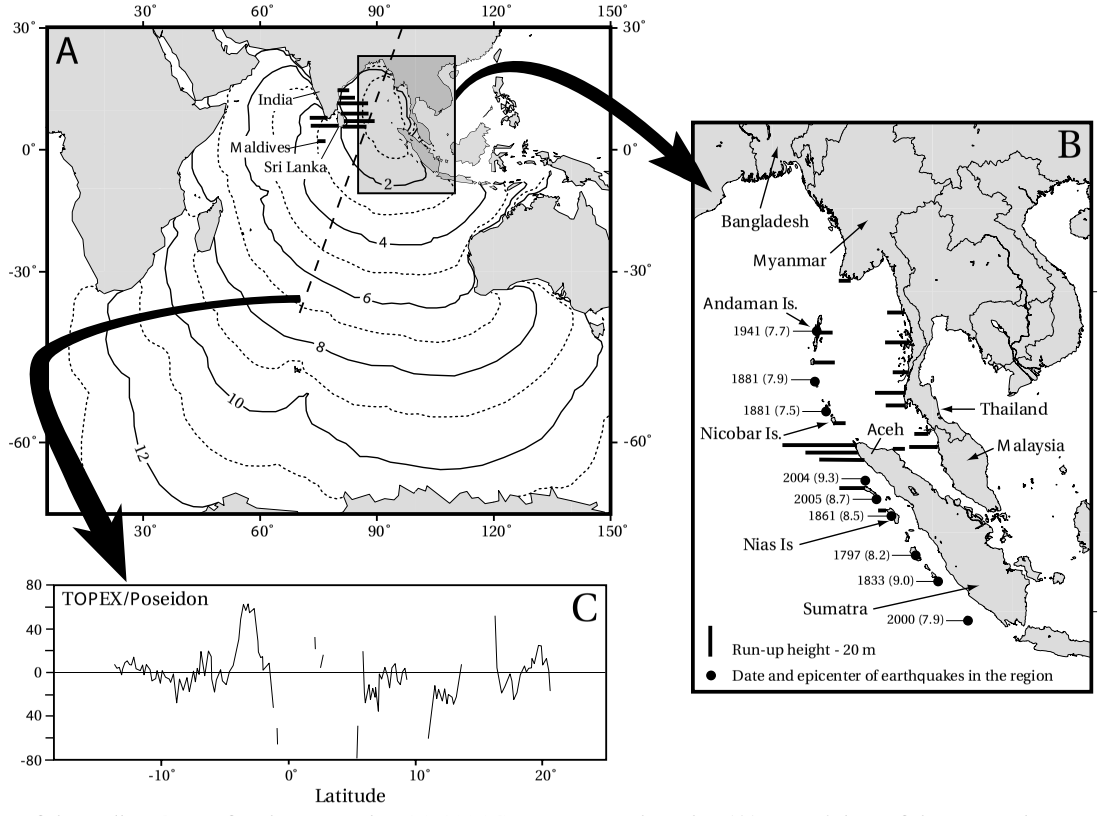

Figure 5.23. Map of the Indian Ocean for the December 24, 2004 Sumatran earthquake. (A) Travel time of the tsunami across the ocean. Based on National Geophysical Data Center (2006a). (B) Location and magnitudes of epicenters of the 2004–2005 earthquakes and previous earthquakes in the region. Based on Subarya *et al.* (2006). (C) Height of the tsunami as measured by the TOPEX/Poseidon satellite 2 hours after the earthquake. Based on National Oceanic and Atmospheric Administration (2006). Run-up heights in (A) and (B) based on Choi, Hong, and E. Pelinovsky (2006).

Table 5.7. Significant tsunami heights for the December 26, 2004 Indian Ocean tsunami registering on world tide gauges.

Ocean	*Country*	*Location*	*Latitude*	*Longitude*	*Max height* (m)
Indian	Australia	Cocos Is.	−12.12	96.88	0.52
		Carnarvon	−24.88	113.67	1.25
		Geraldton	−28.76	114.59	2.05
		Bunbury	−33.35	115.66	1.90
		Hillarys	−31.82	115.73	0.90
		Esperance	−33.87	121.90	0.80
	Thailand	Rangong	9.58	98.38	1.38
		Ta Phao Noi	7.53	98.24	2.22
		Kantang	7.40	99.51	3.20
		Kuah	6.32	99.85	1.80
	India	Chennai	13.10	80.30	1.54
		Kochi	9.96	76.26	1.34
		Paradip	86.70	20.26	3.18
		Tuticorin	78.15	8.80	1.38
		Visakhapatnam	83.28	17.68	>2.58
	Sri Lanka	Colombo	6.93	79.85	2.19
	Maldives	Hanimaadhoo	6.77	73.17	1.98
		Male	4.17	73.50	1.51
		Gan	-0.70	73.17	0.89
	Diego Garcia Is.		−7.28	72.40	0.54
	Oman	Salalah	17.00	54.07	2.55
	Seychelles	Point La Rue	−4.68	55.53	2.86
	Mauritius	Port Louis	−20.15	57.50	2.02
	Kenya	Lamu	−2.27	40.90	0.82
	Tanzania	Zanzibar	−6.15	39.18	0.55
	South Africa	Richards Bay	−28.80	32.08	1.65
		East London	−33.02	27.92	1.35
		Port Elizabeth	−33.97	25.47	2.73
		Mossel Bay	−34.18	22.13	2.60
	Antarctica	Syowa Station	−69.00	39.57	1.00

Source: West Coast and Alaska Tsunami Warning Center (2005),Gusiakov (2006), Nagarajan *et al.* (2006), and Stephenson *et al.* (2006).

Ocean	*Country*	*Location*	*Latitude*	*Longitude*	*Max height* (m)
Pacific	Australia	Portland	−38.33	141.6	0.85
		Spring Bay	−42.55	147.93	0.60
		Port Kembla	−34.48	150.92	0.50
		Rosslyn Bay	−23.17	150.78	0.25
	New Zealand	Jackson Bay	−43.98	168.62	0.65
		Timaru	−44.40	171.27	0.80
		Waitangi, Chatham Is.	−43.95	−176.57	0.50
	Russia	Severo-Kurilsk	50.67	156.17	0.26
	United States	Kahului, Hawaii	20.57	−156.28	0.30
		Kodiak, Alaska	57.40	−152.45	0.26
		Crescent City, Calif.	41.43	−124.13	0.61
		Point San Luis, Calif.	35.15	−120.38	0.53
		Santa Monica, Calif.	34.02	−118.3	0.38
	Mexico	Manzanillo	19.05	−104.33	2.60
	Galapagas Islands	Baltra Is.	0.22	−90.42	0.36
	Peru	Callao	12.05	−77.05	0.68
	Chile	Arica	18.33	−70.18	0.72
		Coquimbo	29.58	−71.27	0.36
		Talcahuano	36.75	−73.02	0.43
Atlantic	France	Concarneau	47.58	−4.05	0.50
		Les Sables d'Olonne	47.15	−2.10	0.29
	Canada	Halifax (NS)	44.73	−63.98	0.43
	United States	Trident Pier	28.40	−80.60	0.34
	Puerto Rico	Punta Guayanilla	17.97	−66.75	0.30
		Magueyes Island	58.05	−67.05	0.75
	Brazil	Rio de Janeiro	−22.53	−43.17	1.00
	Falkland Is.	Port Stanley	−51.75	−57.93	0.45
	South Africa	Simons Bay	−34.18	18.43	0.80
		Cape Town	−33.07	18.43	0.96
		Saldanha	−33.02	18.97	0.85
		Port Nolloth	−29.25	16.87	0.50
	South Orkney Is.	Signy	−60.72	−45.60	0.52
	Antarctica	East Ongul Island	−69.00	−39.57	0.75

Africa via the southwest Indian Mid-Ocean Ridge and then north into the Atlantic via the Mid-Atlantic Ridge. Larger heights were measured at Callao, Peru 19,000 km away in the Pacific Ocean than on the Cocos Islands lying 1,700 km southwest of the epicenter in the Indian Ocean—68 cm vs. 52 cm. The pathway to Callao again was via mid-ocean ridges. Energy was also trapped on continental shelves and transmitted parallel to coasts. Crescent City, California, on the west coast of the United States, more than 23,000 km from the source of the tsunami, registered a height of 61 cm.

The enormity of the tsunami generated the most intense research effort for such an event in history. Dozens of experts took to the field to document the evidence, measuring run-up at 965 sites throughout the northwest Indian Ocean where the tsunami was most destructive. The tsunami generated some of the greatest run-ups ever recorded (Table 5.8, Figure 5.23). At Banda Aceh, run-ups exceeding 20 m were measured at ten sites. The greatest run-up reached 50.9 m at Labuhan. This height has only been exceeded four times previously—Indonesia in 1674 (80 m), Kamchatka in 1737 (63 m), and Japan in 1741 (90 m) and in 1771 (85.4 m). Run-up heights approaching 20 m were recorded in Thailand. On the flat coastal plains of Sri Lanka, and on the east coast of India, run-ups reaching 11.3 m and 11.5 m, respectively, swept up to a kilometer inland. Here the second wave was the highest and backwash was a major factor in the disaster as it scoured out channels, and carried people and debris out to sea. Table 5.9 shows the greatest distance inland that the tsunami traveled. This amounted to 5 km in Banda Aceh close to the fault line and up to 1.5 km in India 2,000 km away. In the Maldives, the height of the tsunami exceeded 4.0 m. This was high enough to overwash totally most islands, so that the distance of flooding inland became irrelevant. Flow velocities at Banda Aceh ranged between $5\,m\,s^{-1}$ and $8\,m\,s^{-1}$. The maximum velocity was estimated to be $16\,m\,s^{-1}$.

The tsunami's impact in the region was horrific. For the first time, modern communications and the availability of video cameras in the hands of thousands of tourists brought the disaster into living rooms almost as it happened. Shortly after the waves swept into Galle, Sri Lanka, they were broadcast on TV while the waves were still sweeping across the Indian Ocean to Africa. Despite this instant communication, warnings were futile. The Pacific Tsunami Warning Center in Hawaii at first did not realize the magnitude of the event because automatic computer algorithms were tuned to shorter seismic wavelengths and yielded an initial M_w magnitude of 8.0. When it was realized that this was grossly underestimating the size of the event, there was no mechanism to warn countries in the Indian Ocean because none of the countries being affected belonged to the Pacific Warning Network. By then it was also too late, the wave had done its worse. Finally, the United States State Department made contact with its embassies in Africa. However, there was no means of warning communities there about the impending tsunami. Fortunately, damage and loss of life in Africa was minimal. The ubiquitous method of communication, the mobile (cell) phone, played a muted role. One resident in Thailand safely witnessed the arrival of the gigantic waves and managed to warn a relative farther down the coast on his mobile phone to flee. Had a warning message automatically been "texted" to mobiles in the region, the death toll outside of Sumatra could have been

Table 5.8. Maximum run-up heights for the December 26, 2004 Indian Ocean tsunami.

Country	*Location*	*Latitude*	*Longitude*	*Max height* (m)
Indonesia	Labuhan	5°72′	95°14′	50.9
Thailand	Ban Thung Dap	9°02′	98°15′	20.0
Malaysia	Pasir Panjang	5°18′	100°19′	7.4
Myanmar	Sann Lan Village	13°56′	98°05′	2.9
Andaman–Nicobar Is.	Passenger Jetty, Little Andaman	10°35′	92°34′	16.5
India	Devanampattinam	11°44′	79°47′	11.5
Sri Lanka	Patanangala Beach	6°21′	81°30′	11.3
Maldives	Fanadhoo, Laamu	1°50′	73°30′	4.4
Madagascar	Faux Cap	−25°34′	45°32′	5.4

Source: Choi, Hong, and Pelinovsky (2006), and National Geophysical Data Center (2006b).

Table 5.9. Maximum distance inland for the December 26, 2004 Indian Ocean tsunami.

Country	*Location*	*Latitude*	*Longitude*	*Max dist.* (m)
Indonesia	Multiple	—	—	5,000
Thailand	Ban Nam Kim	8°52′	98°17′	1,673
Malaysia	Penang Island	5°20′	100°12′	3,000
Myanmar	—	—	—	610
Andaman–Nicobar Is.	Port Blair	11°30′	92°43′	500
India	Cuddalore	11°46′	79°47′	1,500
Sri Lanka	Polhena	5°10′	80°32′	905
Maldives	Kulhudhuffushi	6°37′	73°04′	155

Source: Choi, Hong, and Pelinovsky (2006), and National Geophysical Data Center (2006b).

Table 5.10. Death tolls for the December 26, 2004 Indian Ocean tsunami.

Country	*Fatalities*	*Missing*	*Total*
Indonesia	130,736	37,000	167,736
Sri Lanka	35,322	—	35,322
India	12,405	5,640	18,045
Maldives	82	26	108
Thailand	8,212	—	8,212
Myanmar	61	—	61
Malaysia	69	6	75
Somalia	78	211	289
Tanzania	13	—	13
Seychelles	2	—	2
Madagascar	2	—	2
Bangladesh	2	—	2
Kenya	1	—	1
Total	*186,984*	*42,883*	*229,867*

Source: United Nations, 2006

avoided. Sumatra was simply too close to the epicenter, and the majority of the population too far from high land, to flee to safety within the 20–30 minutes that it took the tsunami to reach the coast. This latter aspect has yet to be addressed in Indonesia where a similar tsunami is forecast to occur in the near future on the southern coast of Sumatra, which has a larger population than Aceh.

Table 5.10 shows the final death toll for the 13 countries where deaths occurred. Because the tsunami propagated outward parallel to the fault rupture, very little of the wave traveled north or south through the Indian Ocean. Only two people died in Bangladesh. The wave also had little impact on the African coast. However, in Sumatra, Sri Lanka, and Thailand, it was a major disaster. The final death toll amounted to 229,866 people, the largest for any tsunami event and one of the greatest for any natural disaster. The biggest death toll occurred in Sumatra where at least 165,000 people died. This tally alone surpasses the death toll for any previous tsunami event. Here, the wave arrived within 20–30 minutes of the earthquake. The tsunami arrived in Thailand at 10:00 AM and had a significant impact upon holiday resorts

where tourists were just starting their day on the beaches. The death toll on these beaches was over 8,000 including Bhumi Jenson, the 21-year-old grandson of the king, King Bhumibol Adulyadej. Thailand, as a result, became the first country in the Indian Ocean to establish afterwards its own tsunami warning system. Forensic identification had to be carried out on 3,750 bodies—the largest number outside wartime. Tourists enjoying a late breakfast captured the most dramatic images on video as the wave crashed into beachside dining rooms, through hotel lobbies, and finally over second-floor balconies. Remarkably, a 10-year-old schoolgirl, Tilly Smith, from the UK, remembered a geography lesson taught to her two weeks beforehand about tsunami and managed to convince her parents and others to flee from the beach because the sea was showing all the signs of such an impending wave. In Sri Lanka and India, the wave arrived between 9 AM and 10 AM. In India, many Hindus were taking a holy dip in the ocean, while Christians had traveled to the seaside town of Vailankanni seeking a religious cure at a local shrine. Hundreds of pilgrims from both religions drowned. Whole villages lost all their children who had raced down to collect fish from the seabed in the drawdown that preceded the arrival of the first wave. Fishing communities were badly hit because fishermen and their families lived on the ocean. Fifteen thousand fishing boats were destroyed. In India, the death toll was 18,000, which is underestimated because India refused foreign assistance and in doing so virtually ignored the plight of its citizens on the Andaman Islands. In Sri Lanka, 35,000 were killed including nearly 2,000 passengers, who were drowned on the *Queen of the Sea*, which was washed from its tracks as it traveled near the coast on the morning the tsunami struck. This is the greatest death toll in any rail disaster. Overall, 70% of the deaths were women and children. More men knew how to swim and could climb trees, while women were more likely to be carrying children or trying to lead the elderly to safety. One and a half million people were made homeless in Sri Lanka alone.

Table 5.10 does not indicate the world impact of the tsunami. It became the greatest natural disaster for Sweden with 543 of that country's nationals killed while on holidays in the region, mainly in Thailand. Sweden proportionally lost four times as many citizens in the tsunami as the United States did in the World Trade Center attack on September 11, 2001. Death tolls for other nationals included 552 Germans, 179 Finns, 150 British, 106 Swiss, and 86 Austrians. Up to five times these numbers were holidaying in the region and affected by the event.

The economic destruction was just as great. Unless a building was built of concrete—and few were—structures were bulldozed flat by the force of the initial wave (Figure 5.24). Theorists found it difficult to model the destructive impact of the wave, because the water had picked up so much debris and mud that its density had increased significantly. Such flows of dense slurry had not been envisaged let alone modeled. Along the west coast of Sumatra, little sign of human habitation was left behind as the wave swept across a coastal plain several kilometers wide and smashed into the backing hills, leaving a tide mark 10 m or more above sea level as the most visual sign of recent inundation (Figure 5.25). Ex-patriots returning to their homes from southern cities told of walking through more than a hundred flattened villages without seeing a sign of life. The livelihoods, economic foundations, and social fabric

Figure 5.24. Total destruction of the urban landscape at Banda Aceh. Only houses and mosques made out of concrete were left standing. *Source:* Guy Gelfenbaum, U.S. Geological Survey. *http://walrus.wr.usgs.gov/tsunami/sumatra05/Banda_Aceh /0730 .html*

Figure 5.25. Site of Seaside Resort Hotel north of Leupueng on the west coast of northern Sumatra. Here the flow depth exceeded 10 m, scouring the soil from hillsides and depositing a mixture of sand, clay, and boulders across the flatter plain. Compare this with the similar landscape produced by Flores, Indonesia tsunami of December 12, 1992 shown in Figure 3.6. *Source:* Guy Gelfenbaum, U.S. Geological Survey. *http://walrus.wr.usgs.gov/tsunami/sumatra 05/Seaside.html*

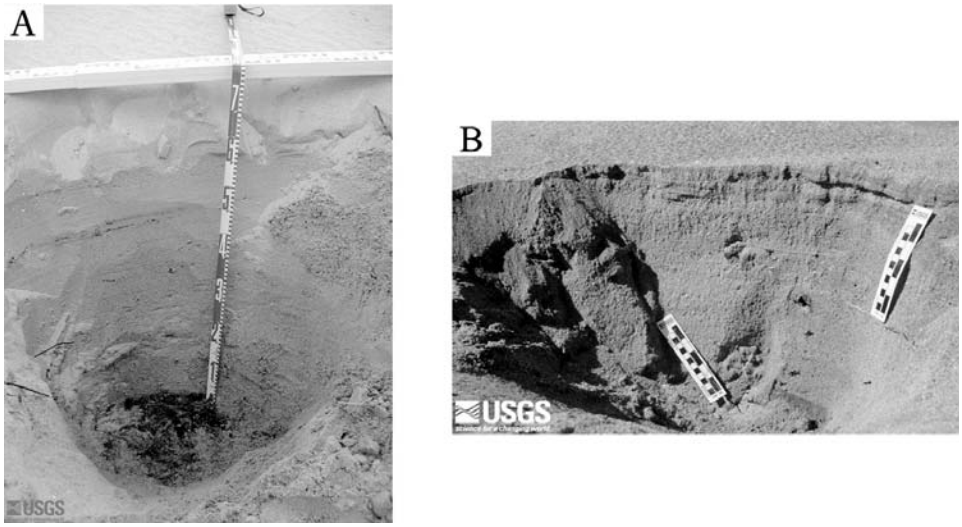

Figure 5.26. Depth of sand layer deposited by the Indian Ocean Tsunami. (A) At Lampuuk on the coast directly west of Banda Aceh, northern Sumatra. The 0.7-meter thickness of the layer is the greatest recorded for an earthquake-generated tsunami. *Source:* U.S. Geological Survey. *http://walrus.wr.usgs.gov/tsunami/sumatra05/Lampuuk/0872html* (B) At Katukurunda on the east coast of Sri Lanka with the greatest exposure to waves. The sand deposit is 37 cm thick. *Source:* U.S. Geological Survey. *http://walrus.wr.usgs.gov/tsunami/srilanka05/Katu5_23 .html*

of a whole generation were destroyed—crops, homes, schools, police stations, and hospitals together with farmers, extended families, teachers, police, nurses, and doctors. The destruction and death toll in Aceh were staggering: 1 million homes, 35,000 hectares of agricultural land, 240 markets, 300 primary schools, 27 police stations, 450 km of roads, 1,057 teachers together with 30,000 schoolchildren, 517 soldiers, and 1,404 police officers with 8,000 members of their families. Over 700 surviving police were so traumatized by the disaster that they did not report for work. Survivors refused to visit the sites of the devastation after dark because they could hear ghosts calling for help. Aceh was left without any established civilian government capable of handling the crisis. Estimates of the socio-economic impact ranged from $15 billion to $80 billion.

The wave also carried significant amounts of sand and mud inland from the shoreline plus thousands of small boulders consisting of coral and cemented beach rock. In Sumatra, coastal retreat amounting to tens of meters occurred with scouring of sediment to depths of 0.5 m–1.0 m being common. In Banda Aceh, a sand layer was laid down as a single massive unit that was 0.7 m thick—thicker than anything previously attributed to a tsunami (Figure 5.26a). The sands often contained angular pebbles and soil rip-up clasts. While the deposits appeared layered, no one-to-one relationship between the number of layers and tsunami waves could be consistently identified. The layering appeared to be a function of variations in flow velocity as the wave moved inland. Backwash also played a role in modifying and redepositing

sediment. In Sri Lanka, the sand layer was 0.37 m thick (Figure 5.26b). Here, the sand deposits could be separated into distinct units representing the passage of more than one wave. Grain size decreased upward in each unit, a facet typical of tsunami deposits. This suffocation of agricultural land by sea sediment, rather than contamination by salt water, was the main cause of decreased soil infertility. However, in Thailand, where significant damaged also occurred, sand layers were so thin and discontinuous that there will probably be little sedimentological indication of the event after the building and tree debris is removed. This has implications for the detection of paleo-tsunami in a country that now believes that it is regularly affected by such events.

Because the disaster was so overwhelming, the destruction so complete, and the recording of the event by tourists and residents so extensive, the response by the international community was unprecedented. Countries made initial pledges of tens of millions of dollars, and moved in their navies and armed personnel to treat the injured, bring food and water to the survivors, evacuate non-residents, and rebuild destroyed communities. This response was initially too little and described as "stingy". It was only when Australia, on January 5, 2005, announced an AUD billion recovery package for Indonesia that other countries began to promise the large amounts of money that would be needed to rebuild countries like Sri Lanka and Indonesia. The public response from around the world was staggering. Many organizations were overwhelmed by the volume of donations and found it difficult to document and receipt them. In several countries, governments had to raise their contributions because their citizens were giving more. Average donations in Australia and Norway reached US$66.4 and $58, respectively. In Australia, the contributions were not only driven by shock, but also by the attitude that Indonesians were neighbors, "We might not agree with them, but when the chips were down, they were as good as the next bloke, and we help them." Australia contributed the highest proportion of Gross National Product, 0.255%. After four months, Oxfam and Médecins Sans Frontières Australia had to publish announcements asking the public to stop giving because they could not find enough projects on which to spend the money. On December 25, 2006, anyone in Sri Lanka or Thailand who said that their country could be devastated by tsunami would have been treated as a pariah. On December 27, they were champions. Tsunami, no matter what the cause, are an underrated hazard.